

國立交通大學

資訊科學與工程研究所

碩士論文

不同的小波分解法對影像壓縮效果的影響

The Influence of Different Wavelet Decompositions on the
Performance of Image Compression

研究生：劉裕泉

指導教授：薛元澤 教授

中華民國九十五年六月

不同的小波分解法對影像壓縮效果的影響
The influence of different wavelet decompositions on the performance of image
compression

研究生：劉裕泉

Student：Yu-Chiuan Liu

指導教授：薛元澤

Advisor：Yuang-Cheh Hsueh

國立交通大學

資訊科學與工程研究所



Submitted to Institute of Computer Science and Engineering

College of Computer Science

National Chiao Tung University

in partial Fulfillment of the Requirements

for the Degree of

Master

in

Computer Science

June 2006

Hsinchu, Taiwan, Republic of China

中華民國九十五年六月

不同的小波分解法對影像壓縮效果的影響

學生：劉裕泉

指導教授：薛元澤

國立交通大學資訊科學與工程研究所碩士班

摘要

小波 (Wavelet) 轉換已經成為近年來影像壓縮的主流，除了最有名的 JPEG2000 採用 DWT 取代傳統的 DCT，也有許多以 DWT 為基礎的影像壓縮演算法，如 EZW，SPIHT，SLCCA，MRMD，等等，都可以達到相當不錯的效果。本篇論文採取類似小波包 (wavelet packet) 的分解方法，將不同類型的影像搭配不同的 wavelet family 做轉換，使影像被分解成數個子頻帶 (sub-band)，再依每個子頻帶的特性，搭配不同的小波係數做進一步的分解。我們也分析與比較了不同的分解層級數，濾波器階數，壓縮率，和不同的影像內容之間的關係，藉由探討這些性質，我們可以決定是否進行子頻帶分解以得到更進一步的壓縮效果。

The Influence of Different Wavelet Decompositions on the Performance of Image Compression

student : Yu-Chiuan Liu

Advisors : Dr.Yuang-cheh Hsueh

Institute of Computer Science and Engineering
College of Computer Science
National Chiao Tung University



In recent years, wavelet transform had become the main stream of image compression. Most famed compression standard JPEG2000 use DWT instead of traditional DCT. Except for JPEG200, there are also many image compression algorithms which are based on DWT, like EZW, SPIHT, SLCCA, and MRMD. They also obtain good performance and results.

This paper uses a decomposition method which is similar to “wavelet packet”. To decompose different images with different wavelets, and further divide high frequency subbands of the original image by the characters of subbands. We also analysis and compare the relationships between the numbers of decomposition, filter orders, compression ratios, and different image contents. By investigating these properties, we can decide whether a subband will be decomposed or not in order to get improved performance.

誌謝

在此感謝我的指導教授 薛元澤教授，在這些日子對我悉心的指導和照顧，教導我做學問的方法，並從他身上學到很多待人處世的道理，讓我畢生受益無窮，以及口試委員 張隆紋教授和 陳玲慧教授，兩位老師不吝指教，使這篇論文更加完善。

我還要感謝王聖博學長，莊逢軒學長，何昌憲學長，王蕙綾學姊，高薇婷學姊，蔡盛同學長於研究上的寶貴建議，並且提供了很多的參考資料。

同窗的佩君，慧瑩，盈賢，仲庭於課業上的研究和討論，在這兩年內與我共同努力，互相砥礪，陪我度過這段快樂的實驗室生活。

謹以此論文獻給我親愛的家人和朋友，我的父母與兄弟，以及所有曾經幫助我的人，感謝你們在這段期間給我的關心，支持與鼓勵，祝福你們永遠健康與快樂。

CONTENTS

ABSTRACT (CHINESE).....	iiii
ABSTRACT (ENGLISH).....	iiiv
ACKNOWLEDGEMENT.....	v
CONTENTS	vi
LIST OF FIGURES	viii
LIST OF TABLES	x
CHAPTER 1 : Introduction	1
1.1 Motivation	1
1.2 Previous Works.....	1
1.3 Organization of this Thesis.....	3
CHAPTER 2 : Background	4
2.1 Transformation Coding.....	4
2.2 Discrete Wavelet Transform (DWT).....	4
2.3 Choice of Wavelet.....	10
2.4 Discrete Cosine Transform (DCT)	16
2.5 Wavelet Image Coding Algorithm.....	17
2.5.1 Image Compression Schemes.....	17
2.5.2 EZW& SPIHT	18
2.6 Image Quality Evaluation.....	20
CHAPTER 3 : Proposed Method.....	23
3.1 System Structure.....	23
3.2 Choose appropriate Wavelet family and Order	23
3.2.1 Number of Decompositions.....	24
3.2.2 Image Content	25

3.2.3 Choice of Wavelet Function and its Filter Order	25
3.3 Decomposition methods	26
3.3.1 Find the adaptability of subband decompositions in different images	26
3.3.2 Advanced subband decomposition of images.....	28
3.3.3 Using different coefficients to subbands	29
3.4 Proposed Method.....	30
3.4.1 Proposed 1 : DWT Based Decomposition.....	30
3.4.2 Proposed 2 : DCT Based Decomposition	33
CHAPTER 4 : Experimental Results.....	34
4.2 Decomposition Levels	34
4.2 Choose appropriate wavelet family for LL subband	36
4.3 The effects of different subbands decomposition on compression performances.....	41
4.4 Advanced subband decompositions.....	50
4.5 Using different filter in subband decompositions.....	53
4.5.1 Using DCT in subband decompositions	53
4.5.2 Using different wavelet filter in subband decompositions.....	55
4.6 Final experimental results	59
CHAPTER 5 : Conclusions and Future Works.....	62
5.1 Conclusions	62
5.2 Future Works	63
References.....	64

LIST OF FIGURES

Fig. 2-1	Structure of wavelet decomposition.....	6
Fig. 2-2	Four subbands of DWT decomposition	7
Fig. 2-3	Level 1 wavelet decomposition of Lena image	8
Fig. 2-4	Level 3 wavelet decomposition of Lena image.	9
Fig. 2-5	Level 3 wavelet decomposition.	10
Fig. 2-6	Scaling functions and Wavelet functions of 5 different Daubechies wavelets:Db1, Db3, Db5, Db8 and Db10.....	15
Fig. 2-7	Three major parts of a lossy image compression scheme.....	18
Fig. 2-8	Child -Parent relationships between pixel and blocks.....	20
Fig. 3-1	The standard procedure of lossy image compression scheme	23
Fig. 3-2	The standard procedure of image reconstruction scheme.....	23
Fig. 3-3	High frequency subband decomposition flow chart	27
Fig. 3-4	Advanced decomposition of HL subband.....	29
Fig. 3-5	Flow chart of DWT based decomposition and compression algorithm.....	31
Fig. 3-6	8-4-2-2-2 DCT Decomposition Method	33
Fig. 4-1	Lena and Baboon	35
Fig. 4-2	LV3 decomposed image and its reconstruct (upper), LV6 decomposed image and its reconstruct (below)	36
Fig. 4-3	Peppers, Barbara, Straw	38
Fig. 4-4	Scaling function and wavelet function of Db1 and 10.....	39
Fig. 4-5	Results of different filter orders in Peppers and Resolution Chart.....	40
Fig. 4-6	LV8 LL subband decomposition	42
Fig. 4-7	Only HL subband decomposition	43
Fig. 4-8	Goldhill and Fruits.....	45
Fig. 4-9	Straw and Boat.....	46

Fig. 4-10	Grass and House.....	48
Fig. 4-11	Airplane and Grass.....	49
Fig. 4-12	Grass and House.....	54
Fig. 4-13	8-4-2-2-2 DCT (left) V.S. Original SPIHT encoder (right).....	54
Fig. 4-14	8-4-2-2-2 DCT (upper) V.S. Original SPIHT encoder (below).....	55
Fig. 4-15	Our proposed (left) can improve some details.....	60



LIST OF TABLES

Table. 2-1	Properties of wavelet families.....	11
Table. 2-2	Filter coefficients of some wavelets	13
Table. 2-3	Performance comparison of the DCT-Based embedded image coder, and the SPIHT coder when a 3-level wavelet transform is used	17
Table. 2-4	Performance comparison of EZW and SPIHT	21
Table. 3-1	Performance comparison of Only 3 Level SPIHT and Standard SPIHT	24
Table. 4-1	Results of Lena Image	35
Table. 4-2	Results of Baboon Image	35
Table. 4-3	Fifteen adaptive wavelets for each image	37
Table. 4-4	Results of 3 subbands decompositions of Lena.....	44
Table. 4-5	Results of high frequency subband decompositions of Peppers, Fruits, and Man.....	45
Table. 4-6	Results of 3 subbands decompositions of Barbara	47
Table. 4-7	High frequency subband decompositions of Straw and Boat	49
Table. 4-8	High frequency subband decompositions of Airplane and Grass	50
Table. 4-9	Higher Level LH subband decompositions of Straw with size 256*256.....	51
Table. 4-10	Higher Level LH subband decompositions of Boat with size 256*256.....	55
Table. 4-11	Results of original SPIHT and 8-4-2-2-2 DCT.....	55
Table. 4-12	Barbara at 0.5 bit/pixel high frequency subband	

	decomposition.....	57
Table. 4-13	Only HL subband decomposition of Boat, Goldhill, and House at 0.5 bit/pixel.....	58
Table. 4-14	Final results of Barbara with size 512*512, our proposed and 8-4-2-2-2 DCT and other well-known compression algorithms.....	61



CHAPTER 1

Introduction

1.1 Motivation

In recent years, many studies have been made on wavelets. Image compression is one of the most visible applications of wavelets. Wavelet transform had been a main stream of researches in image compression. JPEG2000 [4], [12] is a new standard of image compression. It uses DWT instead of DCT in past JPEG [11] standard. Except for JPEG2000, there are many image compression algorithms which are based on DWT, like EZW [25], SPIHT [10] [24], SLCCA [9], and MRMD [3]. They also obtain good performance and results.

This thesis uses SPIHT algorithm to compress and reconstruct images and calculate their PSNR values. After DWT, we decompose high frequency subbands of the original image and encode it. The effects of different wavelet families, filter orders and decomposition methods are examined. We will investigate their relationship and find their best combination to improve compression performance.

1.2 Previous Works

This paper is inspired by [1], [2]. Their presented results are based on the idea of wavelet packet of further dividing the low and high frequency subbands respectively. In the wavelet transform, only the low-resolution subband is further decomposed, whereas both the low frequency and high-frequency portions need to be decomposed in the wavelet packet. Decomposing the low and high frequency subbands can enhance performance of “Zerotree” based compression algorithm, like EZW and SPIHT.

Although wavelet packet can further divides high frequency subbands and

enhances compression performance. It costs high time complexity because that the selection of a “best” basis for any particular image may be performed in a number of ways. Coifman *et al.* suggested the use of an additive **cost function** that is applied to each set of parent and child nodes in the pruning process.

In this paper, we do not use a cost function to select the optimal bases, due to its computational complexity. We try to find another method which can decompose high frequency subbands well.

Besides, in [5], [7] and [15], they presented that different wavelet functions, different filter orders, numbers of decompositions, image contents, and compression ratios can influence final compression results. This paper will analysis and compare these results further. After comparing these results, we will combine them with our methods, and apply them in our paper.

In [6], [9] and [22], they present some methods combining DWT and DCT. In [13], [14], the DCT-based coder has lower complexity than wavelet-based coder. The hardware (or software) implementation of the DCT is less expensive than that of the wavelet transform. DCT still has some superiority over DWT. One of our proposed methods also uses DCT to divide image into sub-blocks and combine wavelet-based algorithm to compare with other decompositions.

After different kinds of decompositions, we encode these decomposed subbands or sub-blocks. In [2], [13], and [24], Said and Pearlman described an SPIHT coder that achieves about 1 dB gain in PSNR over Shapiro’s original coder (EZW) at the same bit rate for typical images. We adopt SPIHT as our image compression encoder, and our decomposition methods can enhance the spatial dependency of the original image to enhance the SPIHT encoder’s performance.

1.3 Organization of this Thesis

The remainder of this thesis is organized as follows. In Chapter2, we briefly introduce DWT, properties of different wavelets, DCT, some image compression coding algorithms, and image quality measure evaluation.

In Chapter3, we simply describe our proposed experimental methods in detail. Different decomposition methods, parameters, test images are shown.

In Chapter4, we present our experimental results. Our method will be compare with other famed compression algorithms.

In Chapter5, the conclusions and future works will be stated.



CHAPTER 2

Background

2.1 Transformation Coding

In this chapter, we will introduce two popular transform coding algorithms: DWT and DCT. DCT is a transform in common use, and DWT becomes the main stream of transform coding.

Transform coding is a very important part of image compression techniques. It transforms original signal to another representation. This representation can be inverted to the original signal. After transformation, energies will be more compact than the original signal. They are compressed much easily.

2.2 Discrete Wavelet Transform (DWT)

In recent years, very effective and popular ways to achieve image compression are based on Discrete Wavelet Transform (DWT) and Discrete Cosine Transform (DCT). JPEG [11] is remaining the main aspect of image compression, and MPEG1 and MPEG2 are the main aspects of video compression. They are also based on the DCT transform.

The new image/video compression standards are JPEG2000 [4], [12], and MPEG4. They are based on DWT transform. Many researchers who are active in image coding have been focused on the Discrete Wavelet Transform (DWT) which has become a standard tool in image compression applications because of their data reduction capability.

DWT has a great similarity to subband coding (SBC). DWT uses two different functions to decompose the origin image. They are **wavelet function ψ** and **scaling**

function ϕ .

The wavelet function ψ represents the high frequency which corresponding to the detailed parts of an image, and the scaling function ϕ for low frequency corresponding to the smooth part of an image.

Because we can regard a 2-D image as a 2-D matrix, so we can extend 1-D DWT to 2-D (x,y) coordinate. That is to say $\phi(x,y) = \phi(x) \phi(y)$.

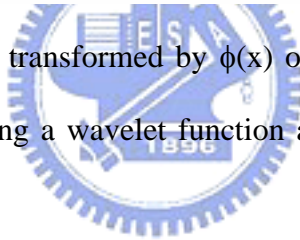
The 2-D wavelet **functions ψ** can be obtained as:

$$\psi_{j,m,n}^i(x,y) = 2^{\frac{j}{2}} \psi^i(2^j x - m, 2^j y - n), \quad i = \{H, V, D\}$$

And 2-D **scaling function ϕ** is

$$\varphi_{j,m,n}(x,y) = 2^{\frac{j}{2}} \varphi(2^j x - m, 2^j y - n)$$

An image can be simply transformed by $\phi(x)$ or $\psi(x)$, or we can obtain a 2-D wavelet function by multiplying a wavelet function and a scaling function. Fig. 2-1 shows the sketch map.



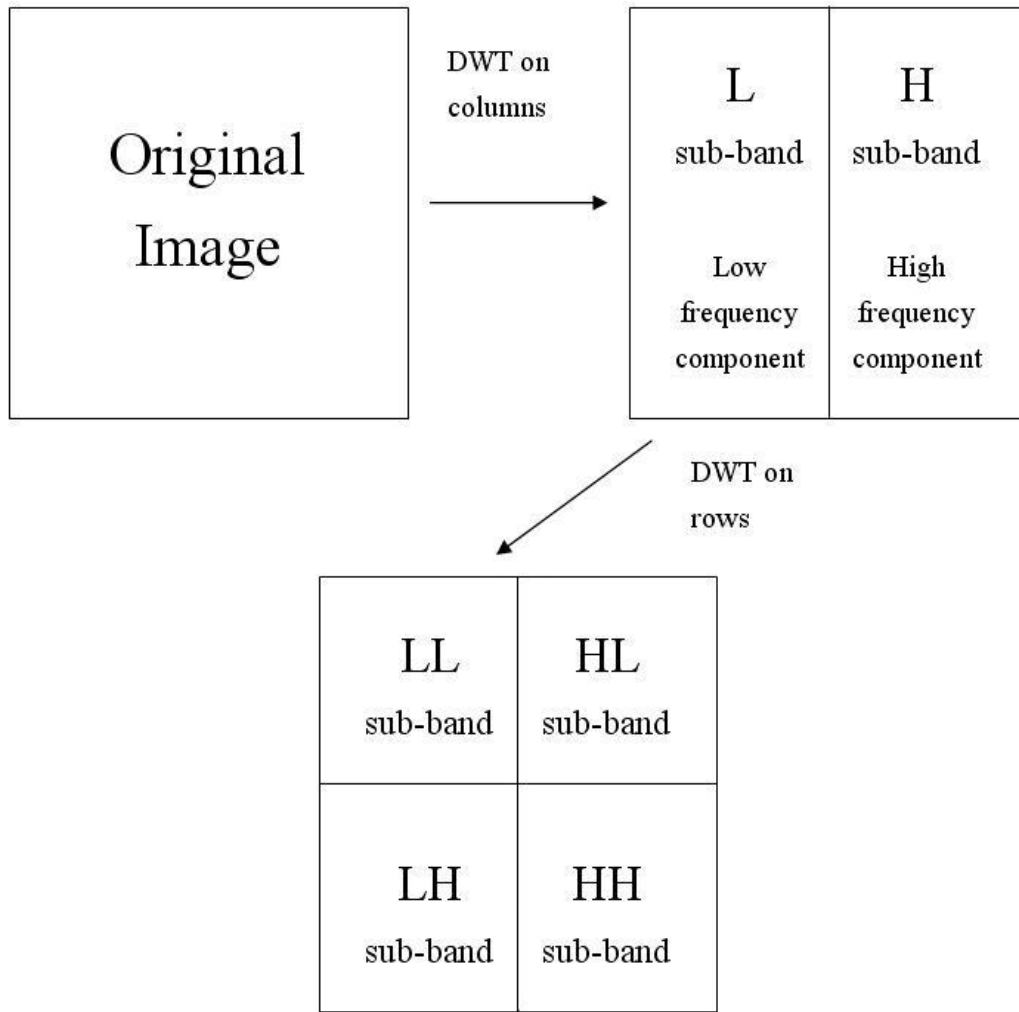


Fig. 2-1. Structure of wavelet decomposition

After Level 1 wavelet decomposition, the original image will be decomposed into four subbands. The left upper image is called “**Approximation**” of the original image (LL subband) .The other three images are “**Details**” of the original one. The right upper image is called “**Horizontal Detail**” of the original image (HL subband) ; The left lower image is called “**Vertical Detail**” of the original image (LH subband) ; The right lower image is called “**Diagonal Detail**” of the original image (HH subband) ; They correspond to 4 wavelet functions as shown in Fig. 2-2

Approximation LL sub-band	Horizontal HL sub-band
Vertical LH sub-band	Diagonal HH sub-band

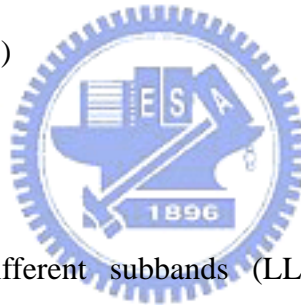
Fig. 2-2. Four subbands of DWT decomposition

Approximation : $\phi(x,y) = \phi(x) \phi(y)$

Horizontal : $\psi_h(x,y) = \phi(x) \psi(y)$

Vertical : $\psi_v(x,y) = \psi(x) \phi(y)$

Diagonal : $\psi_d(x,y) = \psi(x) \psi(y)$



The results in four different subbands (LL, LH, HL, and HH) in the decomposition are corresponding to four types of transformed coefficients.

We show them below:

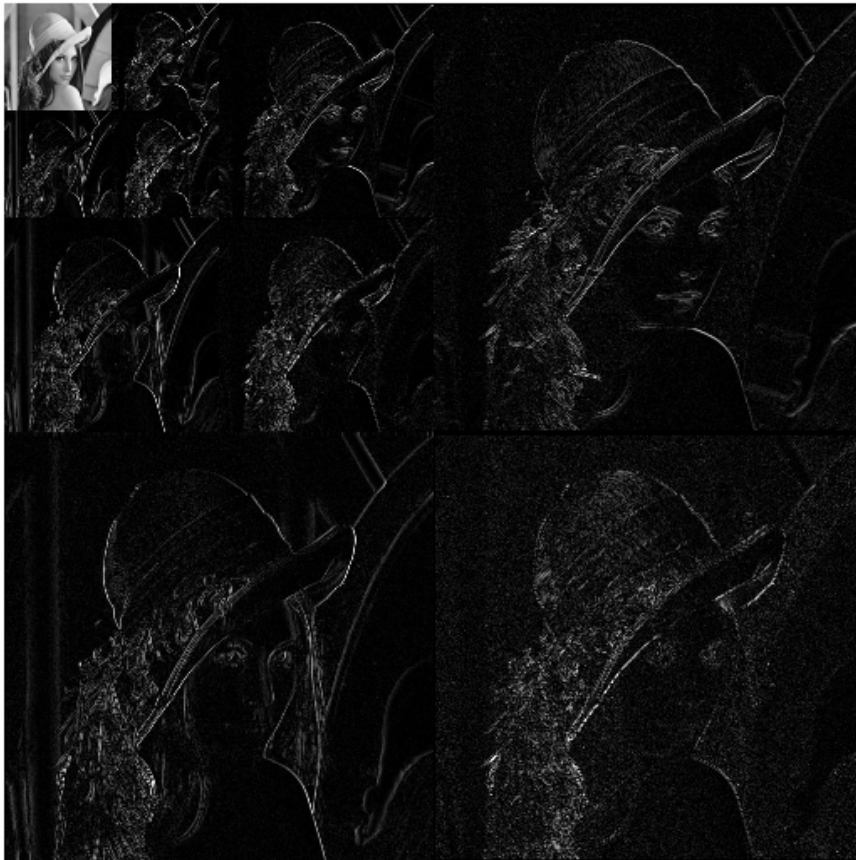
$$W_{\phi}(j_0, m, n) = \frac{1}{\sqrt{MN}} \sum_{x=0}^{M-1N-1} \sum_{y=0}^{M-1N-1} f(x, y) \phi_{j_0, m, n}(x, y)$$

$$W_{\psi}^i(j, m, n) = \frac{1}{\sqrt{MN}} \sum_{x=0}^{M-1N-1} \sum_{y=0}^{M-1N-1} f(x, y) \psi_{j, m, n}^i(x, y), \quad i = \{H, V, D\}$$



Fig. 2-3. Level 1 wavelet decomposition of Lena image

For example, we use DWT to decompose Lena image, and show Level 1 wavelet decomposition of Lena at Fig. 2-3 .Generally speaking, in order to get better performance, we can decompose LL subband again by the same method. Even we use 3 times decomposition at LL subband; we show Level 3 wavelet decomposition of Lena at Fig. 2-4.



LV3 decomposition

Fig. 2-4. Level 3 wavelet decomposition of Lena image

After Level 3 wavelet decompositions, in Fig. 2-5, when we decompose LL subband 3 times, we call other subband LH3, HL3, HH3, LH2, HL2, HH2, LH1, HL1, and HH1. Higher decomposition numbers may be used in order to get advanced performance.

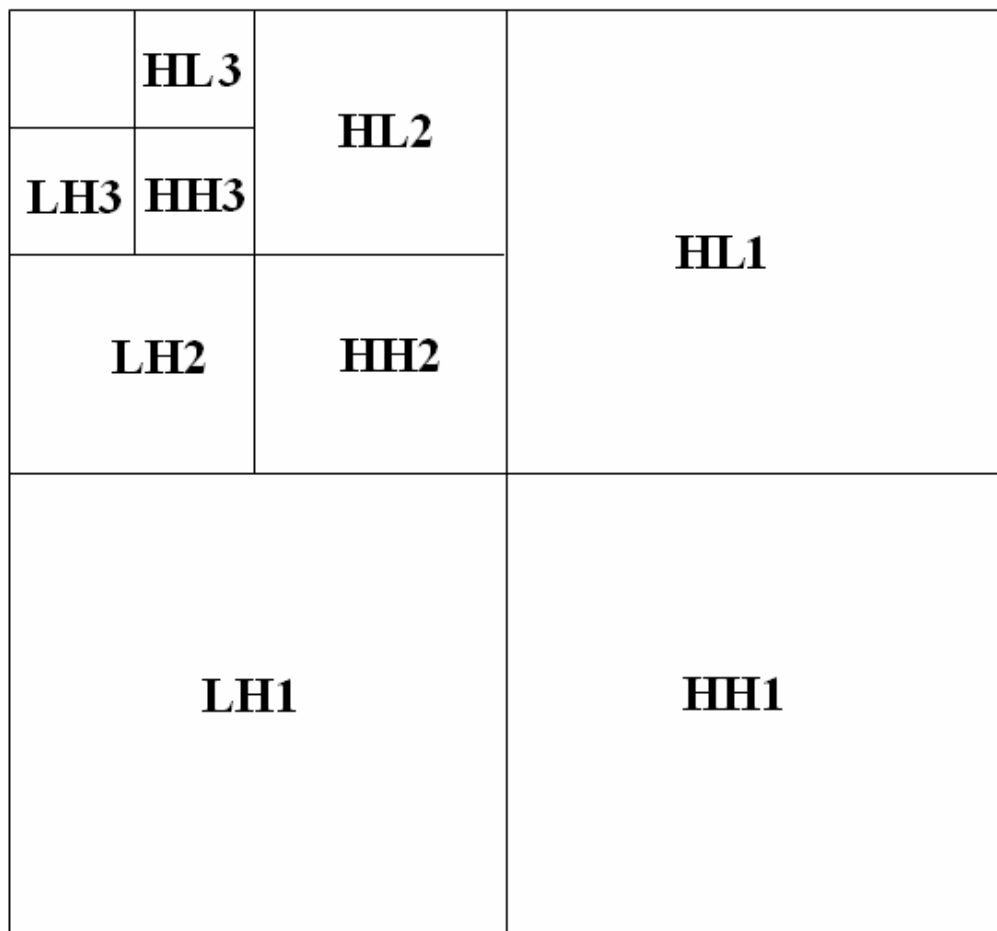


Fig. 2-5. Level 3 wavelet decomposition

2.3 Choice of Wavelet

2.3.1 Wavelet Family

There are many types of wavelet. We choose some families of them in our experiments. They are:

Haar Wavelet (Haar, or called Db1),

Daubechies Wavelet family (Db),

Coiflets Wavelet family (Coif),

Symlets Wavelet family (Sym),

Bi-orthogonal family (Bior),

Reverse-Bi-orthogonal family (Rbio),

"Discrete" Meyer Wavelet family (dmey).

Discussion of wavelet begins at Haar wavelet. The Haar transform is very useful for image because of Haar is one of the simpler wavelet transform which is very useful in codification and problems of image analysis, in addition to be quite fast.

Haar transform has some properties. It is real and orthogonal transformation, and in a vector of $1*N$ the operations can be carried out in $O(N)$. But Haar transform has a poor concentration capacity of the images energy. So we can see poor performance in our later experimental results although Haar is a very effective transformation.

Other properties of wavelet families are showed as Table. 2-1:

Family/Property	Orthogonal	Bi-Orthogonal	Compact support	Regularity	Symmetry
Haar	★	★	★	★	★
Daubechies	★	★	★	poor	asymmetry
Coiflets	★	★	★	poor	near symmetry
Biorthogonal		★	★	★	★
Reverse-Biorthogonal		★	★	★	★
Symlets	★	★	★	poor	near symmetry

Table. 2-1. Properties of wavelet families

By this table, we can see some properties of different wavelet families.

1. **Orthogonal:** Orthogonality can allow fast algorithm
2. **Compact support:** Lead to efficient and fast implementation
3. **Symmetry:** Useful in avoiding dephasing in image processing
4. **Regularity and degree of smoothness:** Related to filter order or length of wavelet filter

Daubechies is asymmetrical, and Coiflets and Symlets are almost (near)

symmetrical, they can cause artifacts at borders of the wavelet subbands.

Symmetry in wavelets can be obtained only if we are willing to give up either compact support or orthogonality of wavelet (except for Haar wavelet, which is orthogonal, compactly supported and symmetric). If we want both symmetry and compact support in wavelets, we should relax the orthogonality and allow non-orthogonal wavelet functions.

The example is the family of Bi-orthogonal and Reverse- Bi-orthogonal wavelets that contain compactly supported and symmetric wavelets. Therefore, non-orthogonality can not use fast algorithm to implement, so Biorthogonal and Reverse- Bi-orthogonal have worse performance than others. It is their main difficulties.

Although Daubechies, Coiflets and Symlets are orthogonal, they all have poor regularity.



2.3.2 Wavelet Filter Order

Each wavelet family can be parameterized by integer that determines filter order. Different filter orders are used inside each wavelet family. Bi-orthogonal wavelets can use filters with similar or dissimilar orders for decomposition (N_d) and reconstruction (N_r). The filter order of Daubechies and Symlets wavelets are positive integers. Haar wavelet uses filter order 1 because Haar = DB1. Coiflets filter orders are from 1 to 5. Higher filter orders. Reverse Bi-orthogonal wavelets have the same situation with Bi-orthogonal wavelets.

From [7], filter with a **high order** can be designed to have good frequency localization, which increases the **energy compaction**. Filters with **lower order** have a better time localization and preserve important **edge information**. In image

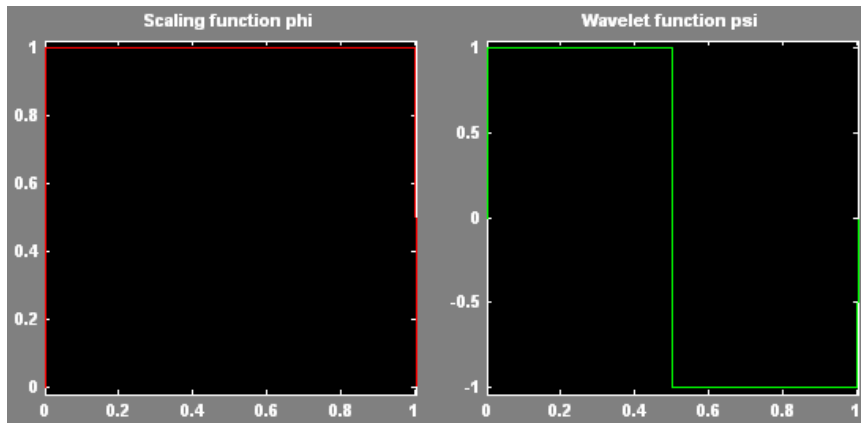
compression application we have to find balance between order of wavelet filter and degree of smoothness, and time complexity.

Inside each wavelet family we can find wavelet function that represents optimal solution related to order of wavelet filter and degree of smoothness but this solution depends on image contents (for different images this optimal solution will not be the same). There are some filter coefficients of some wavelets in Table. 2-2.

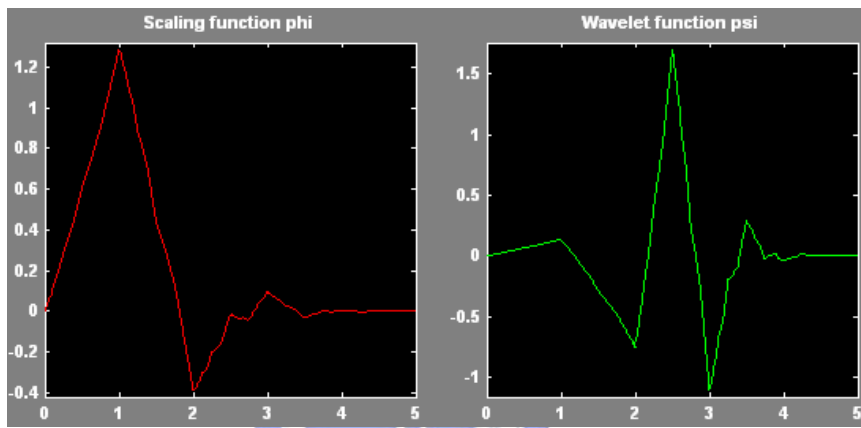
	<i>Db1</i>	<i>Db2</i>	<i>Db5</i>	<i>Coif2</i>	<i>Bior2.2</i>		<i>Bior4.4</i>	
	$a_L(K)$	$a_L(K)$	$a_L(K)$	$a_L(K)$	$a_L(K)$	$s_L(K)$	$a_L(K)$	$s_L(K)$
0	0.0701	-0.1294	0.0033	-0.0007	0	0	0	0
1	0.0701	0.2241	-0.0126	-0.0018	-0.1768	0.3536	0.0378	-0.0645
2		0.8365	-0.0062	0.0056	0.3536	0.7071	-0.0238	-0.0407
3		0.483	0.0776	0.0237	1.0607	0.3536	-0.1106	0.4181
4			-0.0332	-0.0594	0.3536	0	0.3774	0.7885
5			-0.2423	-0.0765	-0.1768	0	0.8527	0.4181
6			0.1384	0.417			0.3774	-0.0407
7			0.7243	0.8127			-0.1106	-0.0645
8			0.6038	0.3861			-0.0238	0
9			0.1601	-0.0674			0.0378	0
10				-0.0415				
11				0.0164				

Table. 2-2. Filter coefficients of some wavelets

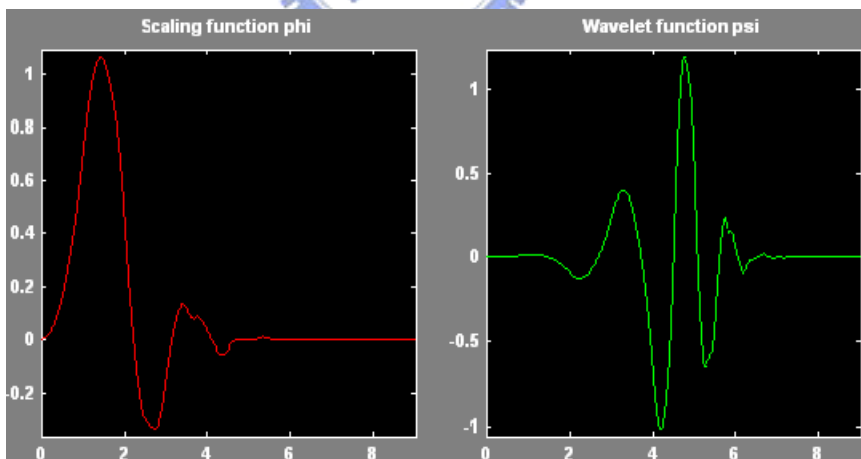
We also design an experiment in Chapter 3 to verify the relationship between image contents and wavelet filter orders. In Fig. 2-6 we show scaling functions and wavelet functions of 5 different Daubechies wavelets. They are Db1, Db3, Db5, Db8 and Db10. We can observe the difference in the different wavelet filter orders.



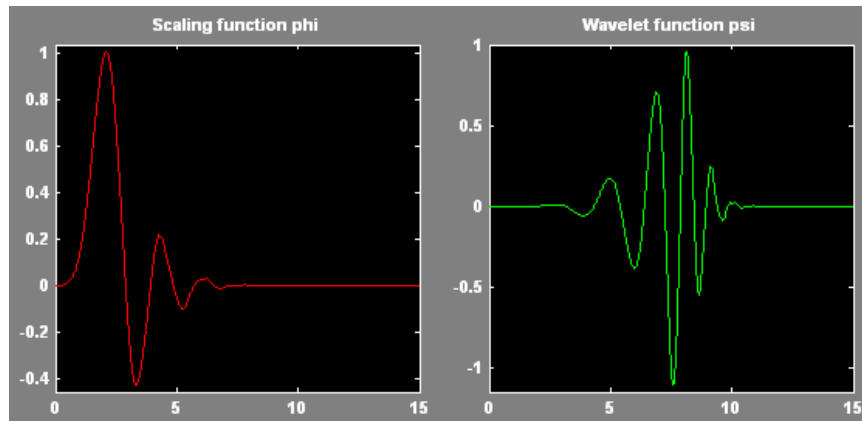
Db1=Haar



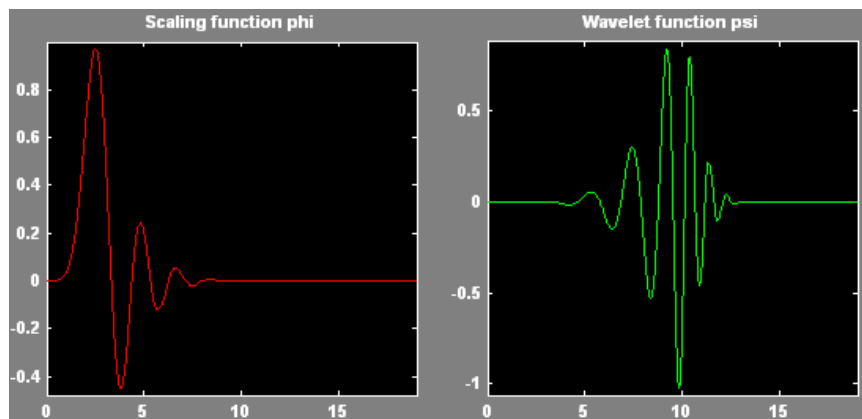
Db3



Db5



Db8



Db10

Fig. 2-6. Scaling functions and Wavelet functions of 5 different Daubechies wavelets: Db1, Db3, Db5, Db8 and Db10

In [16], the appropriate family and filter order for wavelet decomposition have to be chosen ‘adaptively’. We can not find a filter that obtain the best results for all images or for all compression ratios because the performance of a filter is related to the space-frequency features of the image (smoothness, energy, entropy...) and to the compression ratio required.

The wavelet families considered here often compute similar compression results, especially for the Daubechies and Symlets cases, but filter length has to be determined very carefully.

2.4 Discrete Cosine Transform (DCT)

Discrete Cosine Transform (DCT), like DWT, is also a transform. It also can compact energies for convenience of subsequent image compression schemes, like Quantization and Encoding. DCT image transform coding generally divides $N \times N$ size image into $n \times n$ non-overlapped sub-blocks, then it executes unitary transform to each sub-block. The unitary transform is invertible.

Of course, we also can't divide image into $n \times n$ blocks, and use DCT directly to entire image. Without dividing blocks, we can prevent DCT to account for “**Blocking Effect**”. “**Blocking Effect**” is the weakest point of DCT. Taking entire image into DCT will cause very poor performance. So it isn't recommended to such use.

We regard a 2-D image as a 2-D matrix. 2-D DCT formula is:

$$F(u, v) = \left(\frac{2}{N}\right)^{\frac{1}{2}} \left(\frac{2}{M}\right)^{\frac{1}{2}} \sum_{i=0}^{N-1} \sum_{j=0}^{M-1} \Lambda(i) \cdot \Lambda(j) \cdot \cos\left[\frac{\pi \cdot u}{2 \cdot N}(2i + 1)\right] \cos\left[\frac{\pi \cdot v}{2 \cdot M}(2j + 1)\right] \cdot f(i, j)$$

And the corresponding inverse 2D DCT transform is simple $F^{-1}(u, v)$,

Where

$$\Lambda(\xi) = \begin{cases} \frac{1}{\sqrt{2}} & \text{for } \xi = 0 \\ 1 & \text{otherwise} \end{cases}$$

The DCT is related to the Discrete Fourier Transform (DFT). Like DFT, DCT also has fast algorithm “Fast DCT” to implement it. It can be implemented in $O(n \log n)$ time complexity. In 2-D $n \times n$ image, it becomes $O(n^2 \log n)$. But DCT doesn't produce extraordinary high frequency coefficients. It can keep high transform performance, and fewer blocking effects than DFT. Secondly, DCT needs only real number computations. By above advantages, DCT is the widest used transform of image compression. JPEG is still an image compression standard which based on DCT. [6], [8], and [11].

From [13], [14] and [23], when we use DWT instead of DCT, we can get some performance improved, no matter DWT is used at image or video compression. See Table. 2-3[3], we can see the performance comparison of the DCT-Based embedded image coder, and the SPIHT coder [24] when a 3-level wavelet transform is used.

For still-image coding, the difference between the wavelet transform and the DCT is less than 1dB, and it is even smaller for video coding. But the DCT-based coder has lower complexity than wavelet-based coder. The hardware (or software) implementation of the DCT is less expensive than that of the wavelet transform. DCT still has some superiority.

Rate (bit/pixel)	PSNR(dB)			
	SPIHT with 3 -level wavelet		Embedded DCT (8*8 DCT only)	
	Lena	Barbara	Lena	Barbara
0.125	30.13	24.16	28.50	24.07
0.25	33.53	27.09	32.27	26.93
0.5	36.90	31.07	35.98	30.87
0.75	38.86	34.00	38.04	33.73
1.00	40.23	36.17	39.06	36.08

Table. 2-3. Performance comparison of the DCT-Based embedded image coder, and the SPIHT coder when a 3-level wavelet transform is used

2.5 Wavelet Image Coding Algorithm

2.5.1 Image Compression Schemes

The goal of image compression is to represent an image as accurately as possible by using the fewest numbers of bits. They are two kinds image compression scheme: lossy and lossless.

The key point of this paper is lossy image compression. In a lossy compression scheme, there is some distortion between the original image and the decompressed

image. The image compression algorithm should achieve a tradeoff between compression ratio and image quality. Higher compression ratios will produce lower image quality and vice versa. Quality and compression performance can also vary according to input image characteristics and content.

A lossy image compression scheme typically has three major parts: Transform, Quantization, and Encoding. Fig. 2-7 shows its flow chart. If we want to get the original image, we just apply the reverse above procedures in a reverse order.

But, only data transformation can't reach the goal of image compression. Transformation may decrease the correlation and redundancy of original data, and compact most energies to fewer transformed coefficients. Because of the total amount of energy before the transformation is equal to that after transformation. After transformation, most coefficients only have less energy. We can achieve the purpose of energy compacting. Image will be really compressed by after Quantization and Encoding.

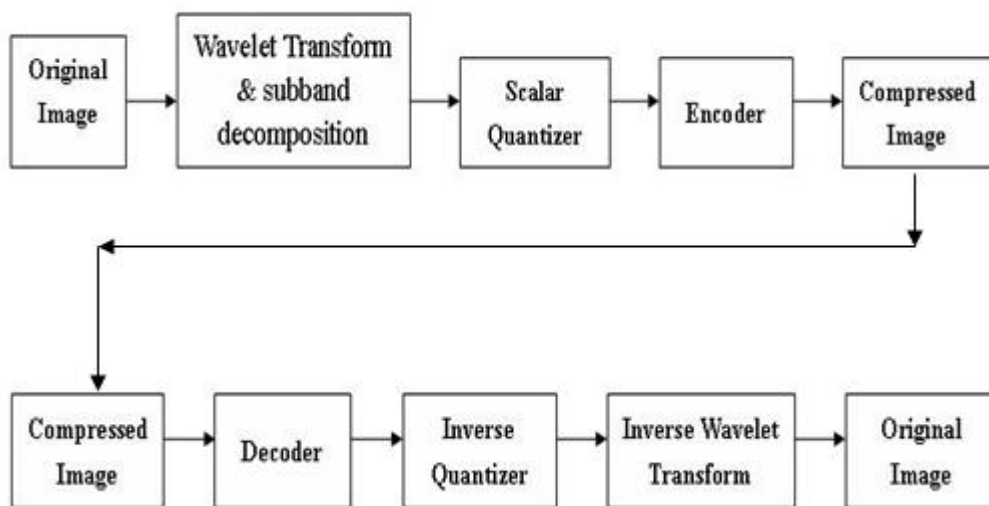


Fig. 2-7. Three major parts of a lossy image compression scheme

2.5.2 EZW & SPIHT

There are some image coding methods based on wavelet transform, such as EZW,

and the enhancement version of EZW called SPIHT [24], MRMD [3], SLCCA [9]...etc. EZW is developed by Shapiro at 1993. This method expands many techniques, and it influences deeply other continually proposed image compression methods.

Firstly, we introduce “EZW” coding method. After wavelet transform, the coefficients of high frequency parts are less than the coefficients of low frequency parts in a decomposed image. To take Haar wavelet transform for an example. When we use the simplest DWT method “Haar” to decompose an image, the coefficients of low frequency parts are got by the result of adding pixel values constantly. By the same way, the coefficients of high frequency parts are got by the result of subtracting pixel values constantly. The coefficients of low frequency can get blurred version of the original image, and the smaller coefficients represent the high frequency parts of the image. They can describe details of the image, and enhance low frequency parts to make the image clearer. Many image compression algorithms use this property and develop a concept called “Zerotree”. EZW [25] also adopted the concept of “Zerotree”.

“Zerotree” method sets up the “**threshold**” value to quantize the coefficients. If the coefficients are greater than threshold value, they can be considered as **significant coefficients**, quite the other way, they are **insignificant coefficients**. If we use the higher compression rate, threshold value is larger, and numbers of the insignificant coefficients will be more, coefficients will be also omitted more. On the contrary, when we use lower compression rate, most coefficients will be preserved.

Besides, EZW has better compression performance than other zerotree quantizers. It is because that EZW can exploit the spatial dependencies of pixels in different subbands of a scalar wavelet transform. There exists a spatial dependence between pixels in different subbands in form of **Child -Parent relationship**.

See Fig. 2-8. There are Child -Parent relationships between small black pixel and 4 x 4 blocks, and 4 x 4 blocks also have relation to 16 x 16 big blocks.

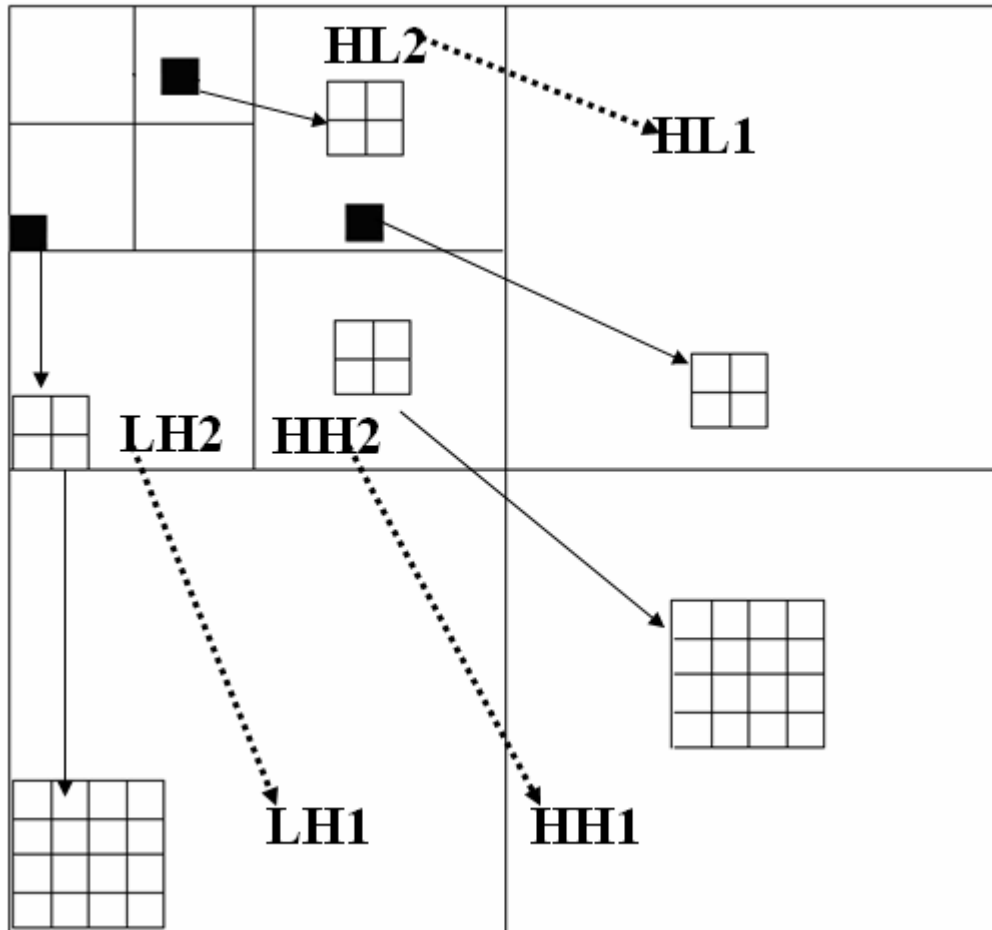


Fig. 2-8. Child -Parent relationships between pixel and blocks

So, we can expand the relationship between pixel and blocks to subband and subband. HL1 subband has Child -Parent relationship to HL2 subband. Other subbands also correspond to each other. HH2 subband corresponds to HH1 subband in spatial location, similarly, we can find that LH2 subband corresponds to LH1 subband in spatial location, and HL2 subband corresponds to HL1 subband in spatial location.

The importance of Child-Parent relation on quantization is that if Parent coefficient has greater value, Child coefficient usually has greater value; if Parent

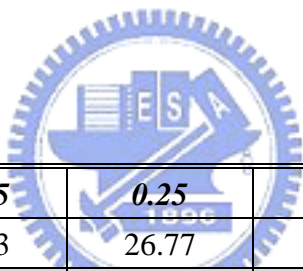
coefficient has smaller value, Child coefficient usually has smaller value.

Because EZW has good spatial dependency, it has good compression performance. SPIHT is an enhance version of EZW, it can achieve about 1dB PSNR over original EZW coder at same bit rate for typical images. SPIHT has more advantages and improvements than EZW, like:

Special symbol for the significance/insignificance of child nodes of significant parent;

Better wavelet filters;

Separation of the significance of child (direct descendant) nodes from that of the grandchild nodes...etc, such that SPIHT can get more effects than EZW, we can see it by Table. 2-4 [3]. Testing image is Barbara. This thesis use SPIHT image compression algorithm.



ALGO\RATE(B/P)	<i>0.125</i>	<i>0.25</i>	<i>0.5</i>	<i>1.0</i>
EZW	24.03	26.77	30.53	35.14
SPIHT	24.86	27.58	31.39	36.41

Table. 2-4. Performance comparison of EZW and SPIHT

2.6 Image Quality Evaluation

The image quality can be evaluated objectively and subjectively. We only use objective methods in this paper. Objective methods are based on computable distortion measures. A standard objective measure of image quality is the reconstruction error.

A standard objective measure of coded image quality is signal-to-noise ratio (SNR) which is defined as the ratio between signal variance and reconstruction error variance [mean-square error (MSE)] usually expressed in decibels (dB)

$$\text{SNR(dB)} = 10 \log_{10} \left(\frac{\sigma_x^2}{\sigma_r^2} \right) = 10 \log_{10} \left(\frac{\sigma_x^2}{\text{MSE}} \right)$$

For the common case of 8 bits per picture element of input image, the peak SNR (PSNR) can be defined as

$$\text{PSNR} = 10 \log_{10} \left(\frac{255^2}{\text{MSE}} \right)$$

Generally speaking, PSNR values are often between 20 and 40. Only one PSNR value is not meaningful in image quality measurement, but the comparison between two PSNR values of two different reconstructed images gives one measure of image quality. We can compare effects of two compression systems by PSNR values.



CHAPTER 3

The Proposed Method

3.1 System Structure

The standard procedure of lossy image compression is showed in Fig. 3-1 .We use wavelet transform to decompose the original image. If we want to get better performance, we may try to decompose the high frequency subband of the original image. Our proposed methods mainly discuss how to decompose subbands of the original image.

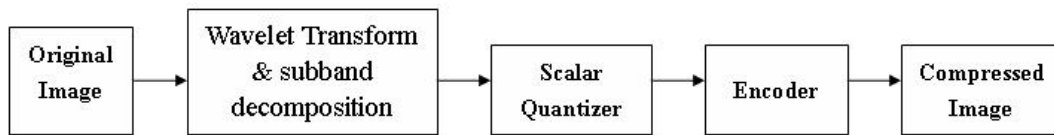


Fig. 3-1. The standard procedure of lossy image compression scheme

This thesis adopts **SPIHT** as Scalar Quantizer and Encoder. We have already introduced SPIHT algorithm at previous chapter. In addition, we can decode the compressed image by reversing the steps in Fig. 3-1, and we can get the reconstructed image. The decoding procedure step is showed in Fig. 3-2.

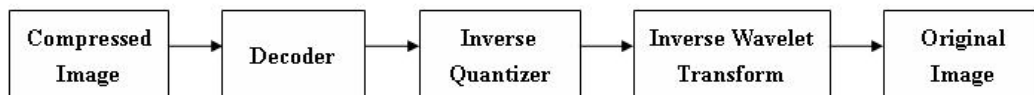


Fig. 3-2. The standard procedure of image reconstruction scheme

3.2 Choose appropriate Wavelet family and Order

From [5], [7], and [15], there are four factors which can influence compression

results. They are: **Number of Decompositions, Image Content, Choice of Wavelet Function, and Wavelet Filter Order or Length.** In this section, we will discuss these four facts separately and try to find the best combination of them.

3.2.1 Number of Decompositions of LL subband

Because SPIHT image compression algorithm has fine spatial dependency, we can decompose the LL subband of the original image many times to get better performance. This is a key feature of SPIHT algorithm. We can see this result at Table. 3-1, the data is proposed by [13]. We design an experiment to verify it and we get the same results in Chapter 4.

Rate (bit/pixel)	Lena		Barbara	
	Only 3 Level SPIHT	Standard SPIHT	Only 3 Level SPIHT	Standard SPIHT
0.125	30.13	31.09	24.16	24.85
0.25	33.53	34.11	27.09	27.58
0.5	36.9	37.21	31.07	31.39
0.75	38.86	39.04	34.00	34.25
1.0	40.23	40.40	36.17	36.41

Only 3 Level SPIHT: the SPIHT coder when a **3-Level** wavelet transform is used.

Standard SPIHT: **Standard** SPIHT image encoder.

All values in the table are PSNR values (dB)

Table. 3-1. Performance comparison of Only 3 Level SPIHT and Standard SPIHT

By this data, we can understand whether compression rate is high or not, more level we decompose the original image, higher PSNR values we get. It is a special character of SPIHT. If we use other compression algorithm, we can't confirm this result.

So we use the results in our proposed methods. Our methods use 8 or 9

decomposition levels to decompose LL subband. If the size of image is 256×256 , we use 8 levels. If its size is 512×512 , we use 9 levels. (Because of $2^8=256$, and $2^9=512$.) More decomposition levels can get better performance.

3.2.2 Image Content

In 3.1, we design an experiment to verify the relationship between the number of decompositions and PSNR values. This section, we will continue our experiments in order to test other three factors.

The sizes of our experimental images are 256×256 and 512×512 . Different image sizes of an image will cause us to get different experiment results.

Experimental images can be classified into three classes: The first class consists of “natural images” which we see in our daily life, for example, Lena, Barbara, Baboon.... The second class is “synthesis images”, like text, artificial images, artificial pictures... The last class is “texture images”. Texture images usually have high complexities; some natural images also have this situation. Images with high spatial activity are more difficult for compression system to handle. They usually have smaller PSNR values than other low spatial activity images, and they are less sensitive to different wavelet families and different filter orders. These images usually contain large number of small details and low spatial redundancy, so we can't compress them easily.

3.2.3 Choice of Wavelet Function and its Filter Order

From [5], [17], [18], [19], we know that the choice of wavelet function is crucial for coding performance in image compression. However, this choice should be adjusted to image content. The compression performance for images with high spectral activity is fairly insensitive to the choice of compression method (for example,

test image Baboon). On the other hand, coding performance for images with moderate spectral activity (for example, test image Lena) are more sensitive to the choice of compression method.

We use many kinds of wavelet families. They are Haar (**Haar, or called Db1**), Daubechies (**Db**), Coiflets (**Coif**), Symlets (**Sym**), Bi-orthogonal (**Bior**), Reverse-Bi-orthogonal (**Rbio**), and "Discrete" Meyer Wavelet family (**dmey**).

They have been introduced in Chapter 2.

Each wavelet family has its adaptable filter order. In our examples, different filter orders are used inside each wavelet family. We have used the following sets of wavelets:

Db-N with $N=1, 2, 3, 4, 5, 6, 7, 8, 9,$ and 10 (among $Db1=Haar$)

Coif-N with $N=1, 2, 3, 4,$ and 5

Sym-N with $N=1, 2, 3, 4, 5, 6, 7,$ and 8

Bior-(n1, n2) and Rbio(n1, n2) with $(n1, n2)=(1,1) (1,3) (1,5) (2,2) (2,4) (2,6) (2,8) (3,1) (3,3) (3,5) (3,7) (3,9) (4,4) (5,5) (6,8)$

And **dmey** is only one fixed filter order.

Our methods will test the influence of 54 different wavelets and image contents when we use them to decompose LL subband of the original image for many times.

3.3 Decomposition methods

3.3.1 Find the adaptability of subband decompositions in different images

Our proposed methods are similar to “Wavelet Packet” [2], [20], and [21]. The wavelet transform often fails to accurately capture high-frequency information, especially at low bit rates where such information is lost in quantization noise. “Wavelet Packet” uses **cost function** to calculate the “**Best tree**” for any particular

image.

Similarly, we decompose LL subband of the original image many times, then we decompose other subbands, like HL1, LH1, HH1.... Energies of other three high frequency subbands will be gathered to upper left corner again. This decompose method can move up the spatial dependency of the image, and enhance the performance of SPIHT algorithm.

Decompose flow chart is revealed in Fig. 3-3

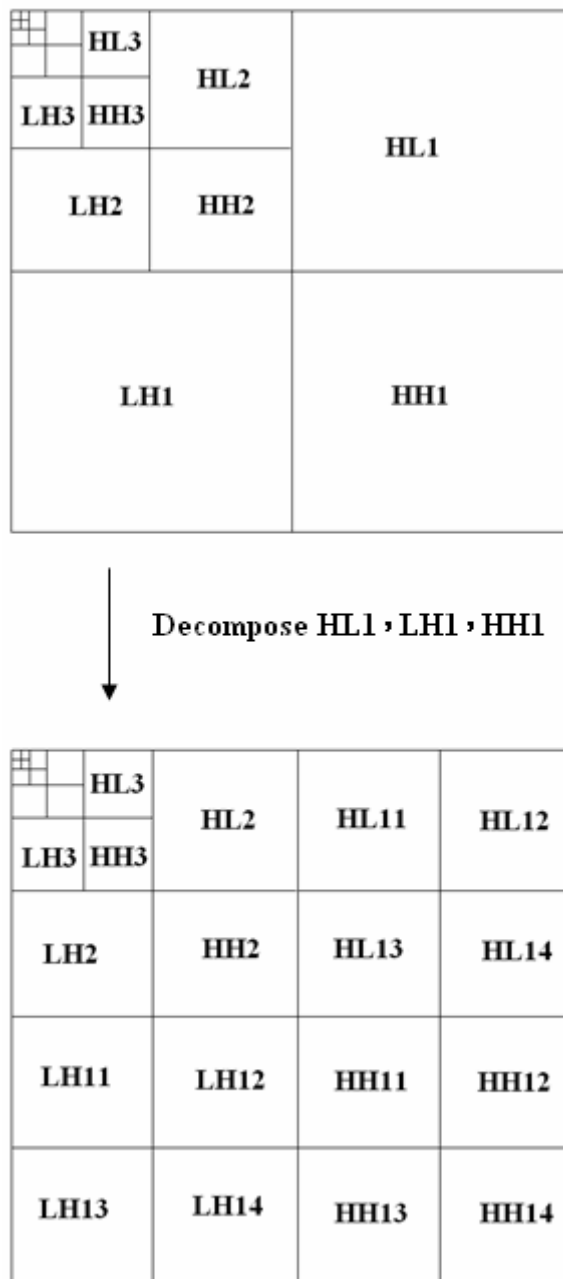


Fig. 3-3. High frequency subband decomposition flow chart

We can find some images which are suit to high frequency subbands decomposition. Some images suit to decompose only one of three subbands and some suit not. We will consider whether an image suits to decompose or not in next chapter.

We can observe the variances from PSNR values to find that the adaptability of subband decompositions of an image is different. Some suit to be decomposed only HL subband, some suit all of three subbands. **We will select these images which are suit to decompose, and we begin the next stage experiments.**

3.3.2 Advanced subband decomposition of images

Referring to the methods of [1], [2], [6], [22]. Observing the wavelet decomposition **Child-Parent relationship** chart, we can find that HL2 is a minification version of HL1 image, LH2 is a minification version of LH1 image, and HH2 is a minification version of HH1 image. They have some resemblances to numerical distribution and some features in statistics. By this special property, we can do this assumption that if we decompose HL1 subband of some image, and we can get better performance, then we decompose its HL2 by the same way, can we get more performance? See Fig. 3-4:

families and orders which can decompose other 3 subbands as well? In other words, if we use Bior6.8 wavelet to decompose a particular image and we get a satisfying result. Can we also use Bior6.8 in other three subbands to get good performance? Or must we use other wavelets? Like Coiflets or Symlets? This experiment will find that wavelet filters which are suit to high frequency subbands. If we can not get satisfying results by using wavelet filters, we will try to use DCT.

3.4 Proposed Method

3.4.1 Proposed 1 : DWT Based Decomposition

Integrating methods which are proposed in previous sections, we combine our methods here. See Fig. 3-5. The compressed data can be decompressed by the inverse order, and get a reconstructed image. Original image and reconstructed image can be used to measure a PSNR value. We will show experimental results in next chapter.



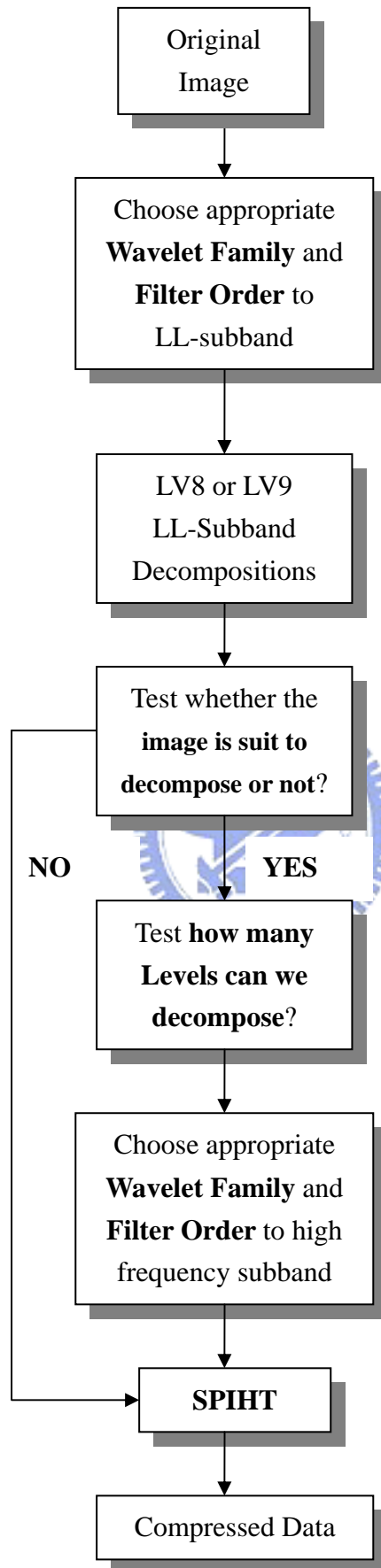


Fig. 3-5. Flow chart of DWT based decomposition and compression algorithm

3.4.2 Proposed 2 : DCT Based Decomposition

Like section 3.4.1, we just modify some steps. We can substitute DWT by using DCT. Our proposed method is similar to [6] and [22]. After LV8 or LV9 LL subband wavelet decompositions, there are still many high frequency subbands. We use DCT instead of DWT to decompose them. HL1, LH1 and HH1 subbands are decomposed by 8*8 DCT, and HL2, LH2 and HH2 are decomposed by 4*4 DCT. And so forth, HL3, LH3 and HH3 are decomposed by 2*2 DCT. By our testing results, we can decompose them to LV5, and the decomposition method can deal with most conditions. Decomposed high frequency subbands also will be encoded by SPIHT, and PSNR values also will be calculated and compared to each other. We call this method “8-4-2-2-2 DCT”. See Fig. 3-6.

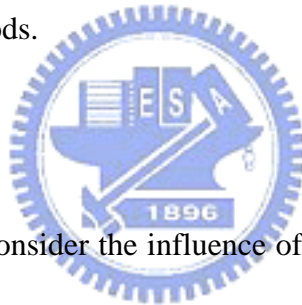


CHAPTER 4

Experimental Results

The sizes of our experimental images are 256*256 and 512*512. If its size is 256*256, we use LV8 LL sub-band wavelet decomposition. If the size is 512*512, then we use LV9 wavelet decomposition in order to get best performance. These images are all 256 gray level images. We take some images as example and list them as below figure.

We use SPIHT as image compression algorithm. SPIHT can quantize and encode coefficients which are decomposed by different wavelet decompositions. The important point of this thesis is to investigate the compression results by using different decomposition methods.



4.1 Decomposition Levels

In this section, we first consider the influence of decomposition levels on PSNR values. From Chapter 3, we can find that more decomposition levels can increase performance of compressions by ascending PSNR values. We can verify this fact by designing a simple experiment. Fig. 4-1 shows **Lena** and **Baboon**. See Table. 4-1 and Table. 4.2 for the results of Lena and Baboon images.

Our experimental images are size 256*256, so the maximum level which we can use is LV8. From this data, we find that more LL-band decomposition levels can cause higher PSNR value. It is because the spatial dependence of SPIHT. This result is the same as the authoritative data.



Fig. 4-1. Lena and Baboon

Rate/PSNR	LV3	LV6	LV7	LV8
<i>0.1</i>	10.9826	25.603	25.6922	25.7232
<i>0.25</i>	20.1341	29.3274	29.3961	29.4181
<i>0.5</i>	25.5311	33.2557	33.2992	33.3104
<i>0.8</i>	30.9334	36.9003	36.9353	36.9421
<i>1</i>	33.2906	38.8017	38.8306	38.8457

Table 4-1. Results of **Lena**

Rate/PSNR	LV3	LV6	LV7	LV8
<i>0.1</i>	10.6281	22.3715	22.4377	22.44923
<i>0.25</i>	19.1886	23.8807	23.9190	23.92807
<i>0.5</i>	22.3737	25.7167	25.7522	25.76114
<i>0.8</i>	24.7925	27.8218	27.8488	27.8565
<i>1</i>	26.2175	29.0434	29.0673	29.0738

Table 4-2. Results of **Baboon**

Fig. 4-2 shows the decomposed subbands and their reconstructed images. Rising PSNR values also get more clear images. Upper half of Fig. 4-2 is LV3 decomposed image and its reconstruct at 0.5 bit/pixel (PSNR=22.37), below half is LV6. (PSNR=25.76)

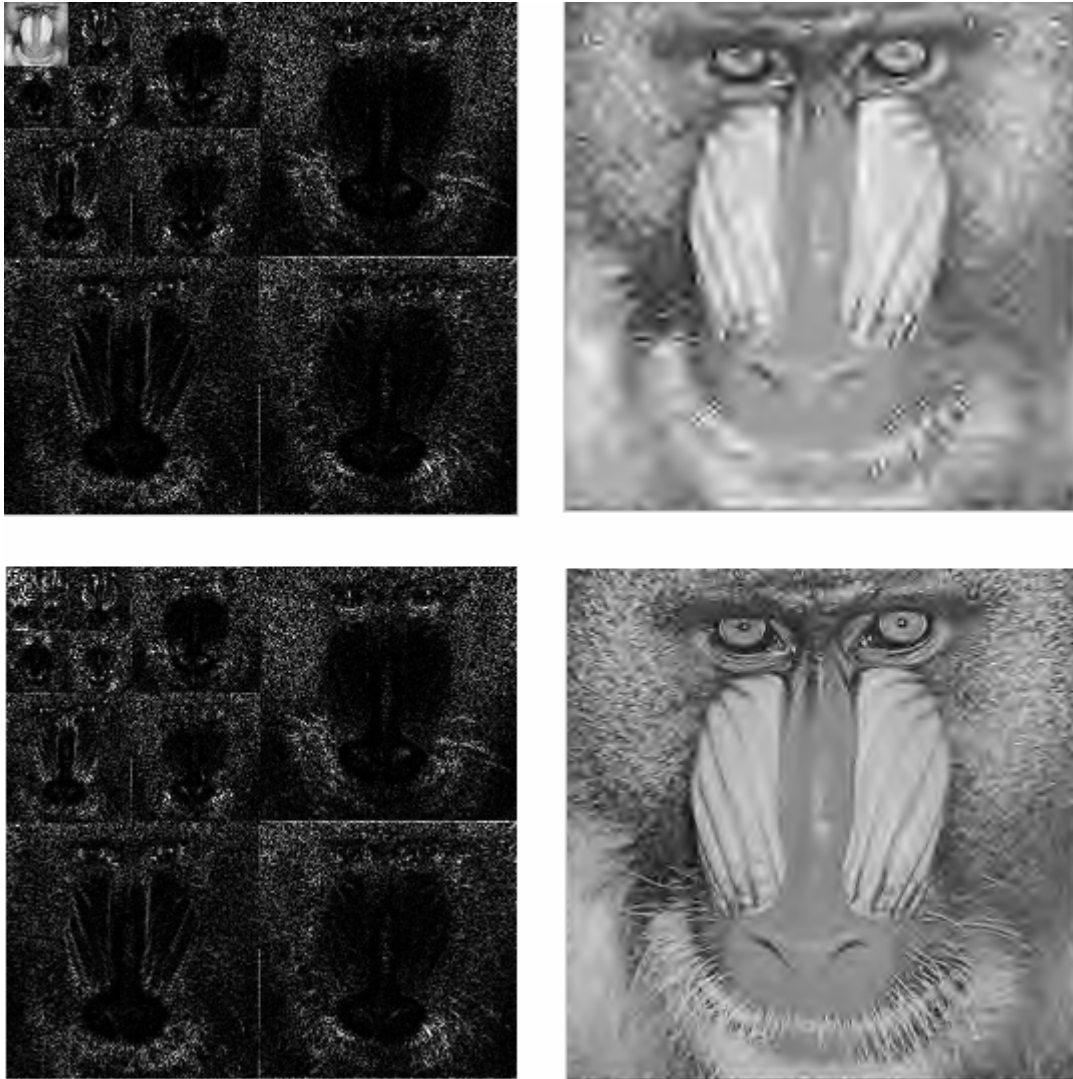


Fig. 4-2. LV3 decomposed image and its reconstruct (upper half), LV6 decomposed image and its reconstruct (below half)

4.2 Choose appropriate wavelet family for LL subband

We use about 20 different images varied from all three classes to proceed our experimental. They are decomposed by different wavelet families and filter orders. We also consider some facts like compression ratio and image size. The results are showed in Table. 4.3.

Wavelet families and their filter orders used in this thesis have been listed in **Section 3.3.2**. There are 54 wavelets. In Table. 4-3, we only list first fifteen adaptive wavelets for each image. Testing images are size 256×256 , and the compression rate is

0.25 (bit/pixel).

Lena		Peppers		Baboon		Barbara		Straw		Resolution Chart	
bior44	29.444	bior68	28.982	bior68	23.928	bior68	27.328	dmey	21.441	db1	22.573
sym8	29.442	sym5	28.920	dmey	23.920	sym5	27.297	bior68	21.410	sym1	22.573
bior68	29.418	sym7	28.903	sym8	23.919	dmey	27.236	db9	21.373	bior11	22.573
coif5	29.351	sym8	28.902	sym7	23.907	sym8	27.225	db10	21.372	rbio11	22.573
sym6	29.333	bior44	28.901	sym6	23.907	bior44	27.223	coif4	21.360	rbio13	22.249
coif4	29.328	coif3	28.889	coif5	23.896	coif3	27.207	sym7	21.358	rbio15	21.762
dmey	29.301	coif5	28.816	coif3	23.884	sym6	27.204	coif5	21.356	bior44	21.743
sym5	29.280	sym6	28.790	sym4	23.878	coif5	27.184	sym8	21.345	sym5	21.692
sym7	29.230	coif4	28.773	sym5	23.867	sym7	27.159	coif3	21.330	db3	21.565
coif3	29.223	dmey	28.769	coif4	23.856	coif4	27.149	sym5	21.329	sym3	21.565
coif2	29.191	coif2	28.729	bior44	23.836	rbio15	27.044	db8	21.310	bior68	21.549
sym4	29.190	sym4	28.683	coif2	23.833	sym4	27.026	db6	21.306	sym7	21.499
rbio15	29.183	db4	28.648	db7	23.798	coif2	27.016	sym6	21.284	sym4	21.485
rbio13	29.134	bior24	28.642	rbio13	23.786	rbio13	26.984	db7	21.278	sym6	21.401
db7	29.104	rbio15	28.634	db5	23.784	db9	26.963	bior44	21.277	sym8	21.366

Table. 4-3. Fifteen adaptive wavelets for each image

We show other 4 images in Fig. 4-3. These testing images are **Peppers, Barbara, Straw and Resolution Chart.**

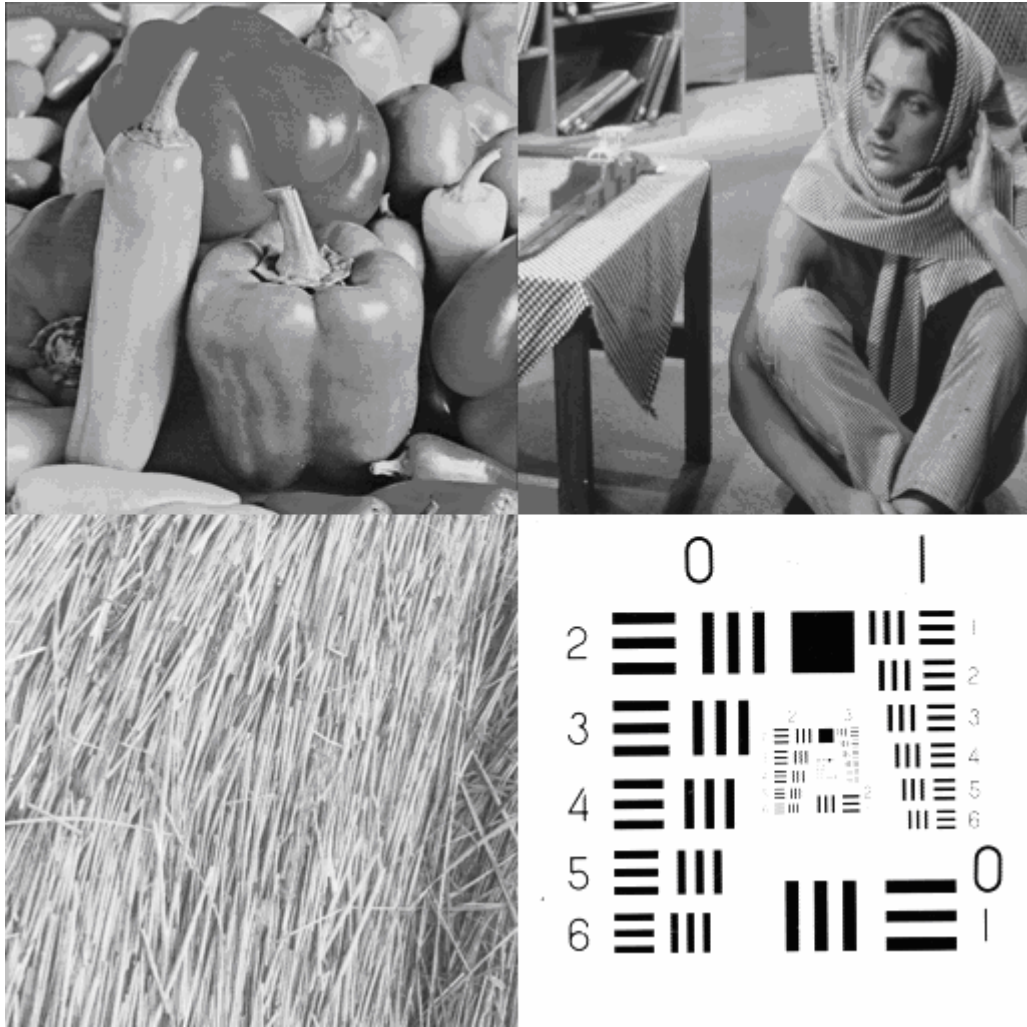


Fig. 4-3. Peppers, Barbara, Straw and Resolution Chart

From this data, our conclusion is similar to [5], [7], and [15]. Natural images have large areas with gradually varying gray level intensities, being therefore well represented by orthogonal wavelet families with smooth basis functions. In general, the family of Bi-orthogonal wavelets work well for most natural and texture images. **Bior 6.8 is the best wavelet can be fit to most conditions.** Synthesis images usually have more texts, triangle, and squares. They are not decomposed well by using smooth basis functions, so we must use **lower filter order** to decompose them. So, **Resolution Chart** image can get better performance by using **filter order 1, like Db1, Sym1, Bior 1.1, Rbio 1.1, Rbio 1.3.**

We show our experiment result to explain these situations. Db1 and Db10

decompose two images: Peppers and Resolution Chart at 0.5 bit/pixel. Observing the wave forms of the scaling functions and wavelet functions of Db1 and Db10, we get anticipant results and data. Fig. 4-4. and Fig. 4-5. Fig 4.4 shows the scaling functions and wavelet functions of Db1 and Db10. Fig. 4-5 show the results of different wavelet filter orders. Fig. 4-5 (a) uses Db1[PSNR=30.3044], (b) uses Db10 [PSNR=32.3071], (c) uses Db1 [PSNR=30.0322], and (d) uses Db10 [PSNR=24.9598]

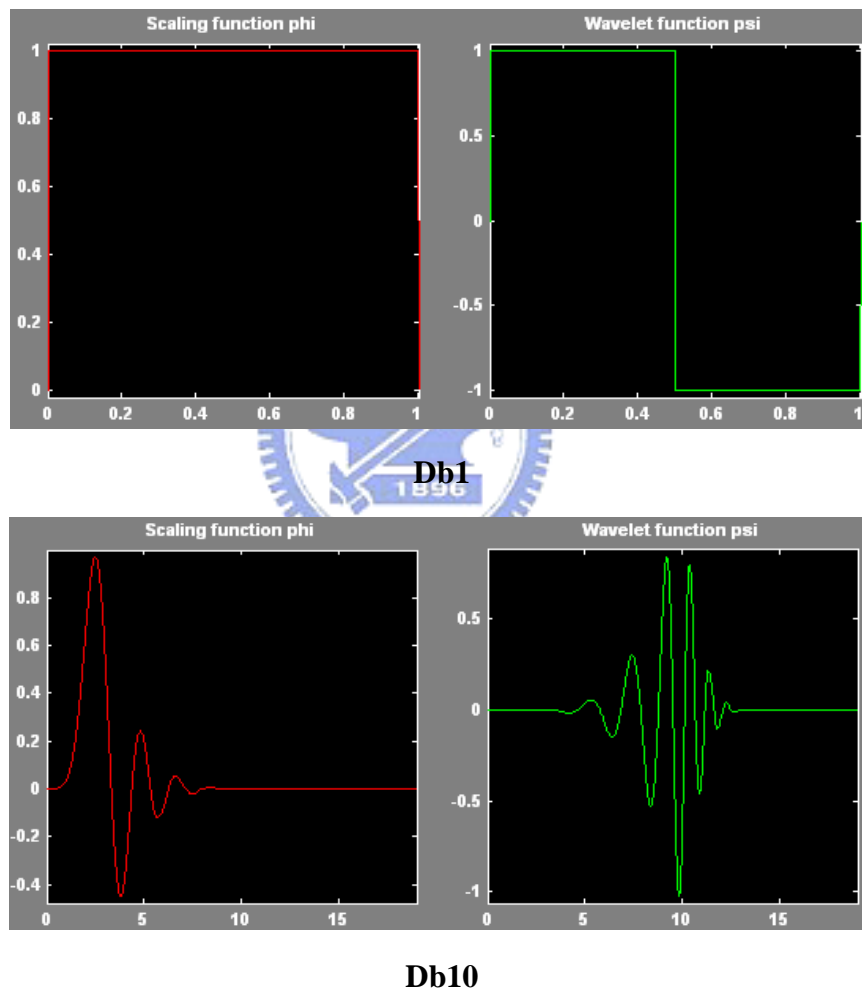


Fig. 4-4. Scaling functions and wavelet functions of **Db1** and **Db10**

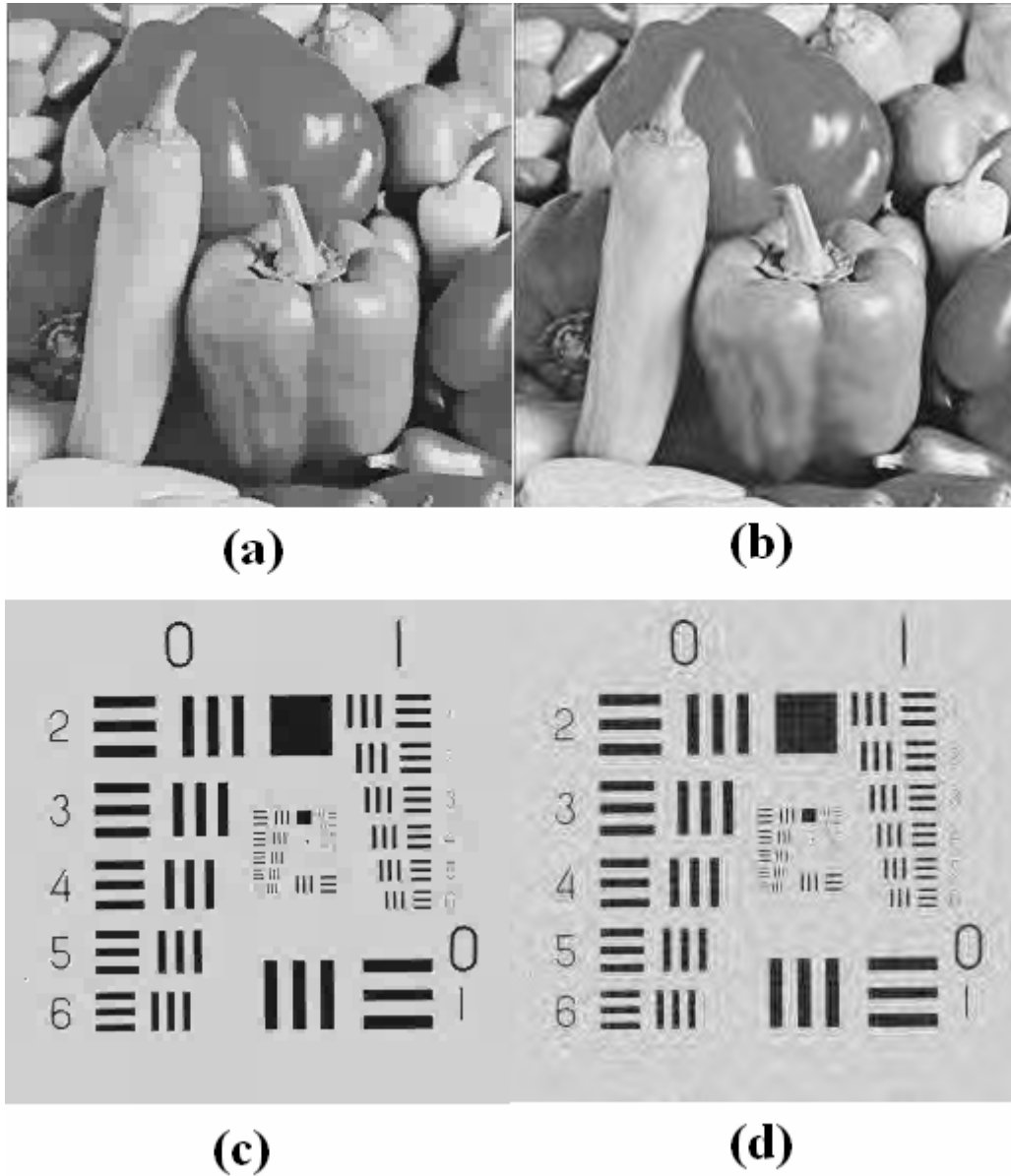


Fig. 4-5 Results of different wavelet filter orders in **Peppers** and **Resolution**

Chart

From this figure, comparing (a)(c) with (b)(d). Fig, 4-5(a) has more artificial contours and blurring parts than (b). Higher filter order causes more energy compaction and gets better effects on most natural images. Fig, 4-5 (c) preserves more edge information than (d) because of lower filter order has better edge information conservation. We know that choose an adaptive wavelet family and related filter orders is very important and the optimal combinations depend on different image

contents.

4.3 The effects of different subbands decomposition on compression performances

From the conclusion of Section 4.1, we know that no matter what compression rate is, LL subband can be decomposed more and more times, in order to get better performance. But it is be restricted by images size. Image with size 512*512 can be actually decomposed at most 9 times. This section will discuss the effects of decomposing HL, LH, and HH three subbands.

Our proposed algorithms are similar to the methods of [1] and [21]. Wavelet Packet has many kinds of decomposition types. Our proposed method will decompose LL subband as more as possible, other three subbands will be decompose or not according to many factors. Such factors as attributes of images, high or low compression rates, and how many high or low frequency parts in the images.... We proposed a simple experiment to observe the results of the 3 subbands decompositions.

In the example, we use images with size 256*256. See details at the flow chart shown in Fig. 4-6

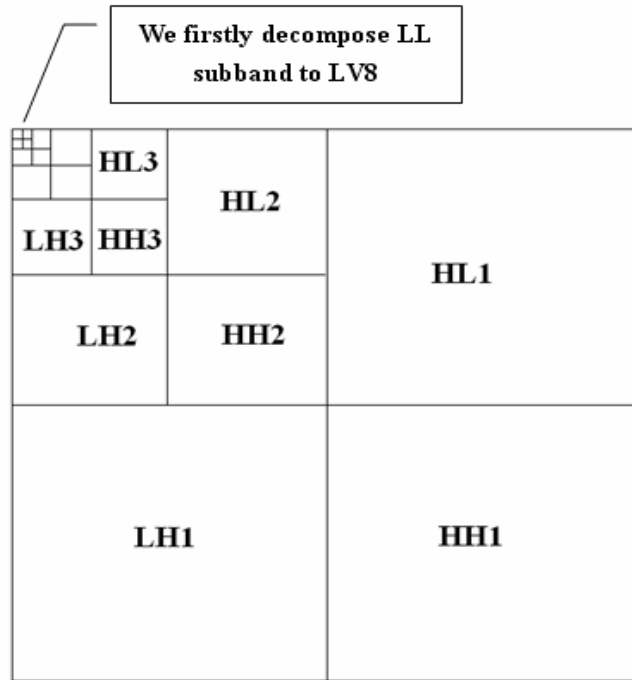


Fig. 4-6. LV8 LL subband decomposition

After decompositions, we survey the results of three subbands decompositions individually, and the results of all three subbands decompositions. In Fig. 4-7, we show the results of **only HL subband decomposition**, the other two subbands and so forth.

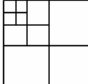
	HL3	HL2	HL11	HL12
LH3	HH3			
LH2		HH2	HL13	HL14
LH1			HH1	

Fig. 4-7. Only HL subband decomposition

We firstly use Lena image with size 256*256 to test subbands decomposition. It is transformed by bi-orthogonal 6.8 filter and its LL subband is decomposed for 8 times.(LV8 LL subband decompositions).Whether compression rate is high or low in Lena image, PSNR values will decrease by any subband decompositions. Higher compression rate causes more loss of the PSNR values. More subbands be decomposed, more PSNR values will be descended. See results in Table. 4-4

Image/rate	Lena/0.25				
HL		●			●
LH			●		●
HH				●	●
PSNR	29.418	29.391	29.4419	29.4133	29.4128
	Lena/0.5				
HL		●			●
LH			●		●
HH				●	●
PSNR	33.31	33.23	33.17	33.314	33.108
Image/rate	Lena/0.75				
HL		●			●
LH			●		●
HH				●	●
PSNR	36.4048	36.1893	36.6154	36.3771	35.9954
	Lena/1				
HL		●			●
LH			●		●
HH				●	●
PSNR	38.8456	38.508	38.51	38.7	38.1517

Table. 4-4. Results of 3 subbands decompositions of **Lena**

These appearances also exist in many natural images.

Except for Lena images, we also find some simpler images, (They have many low frequency parts and simple edges.) like **Fruits** (Fig. 4-8 right), **Peppers** (Fig. 4-9 left), and **Man** (Fig. 4-9 right)...etc. They are not suit to the subband decompositions.



Fig. 4-8. **Goldhill** and **Fruits**

We list parts of their experimental data. See Table. 4-5 for results of Peppers, Fruits, and Man .They are usually simpler images which have more low frequency parts and more smooth zones. Any one of subband decomposition will cause PSNR values to decrease.

Image/rate	Peppers/0.5				
HL		●			●
LH			●		●
HH				●	●
PSNR	33.29	33.12	33.18	33.26	33.01
Image/rate	Fruit/0.5				
HL		●			●
LH			●		●
HH				●	●
PSNR	32.7838	32.4456	32.4697	32.7726	31.7378
Image/rate	Man/0.5				
HL		●			●
LH			●		●
HH				●	●
PSNR	27.9105	27.72	27.78	27.89	27.6

Table. 4-5. Results of high frequency subband decompositions of **Peppers, Fruits,** and **Man**



Fig. 4-9. **Peppers**, and **Man**

Generally speaking, images which have simple edges and a small number of details are not suit to this method. We often use the **standard deviation** to measure an image. If the standard deviation of an image is smaller, it usually has fewer details, for example, Lena and Peppers. Then, texture images commonly have larger standard deviation.

Simpler images have more low frequency parts and more smooth zones. They are not suit to decompose further. We can also find these similar conclusions in some papers which discuss with “wavelet packet.”

But, there exist many natural images which are suit to subbands decomposition. From [2], we know that wavelet packet perform significantly better than wavelets for compression of images with a large amount of texture such as the commonly used Barbara image.

By our experimental results, the Barbara image extremely fit subbands decomposition. Any one of three subbands-HL, LH, and HH of Barbara image can be decomposed well by most wavelet filters. All three subbands can get better performance in any compression rates, as long as we use appropriate wavelet filters to

decompose them.

In Table. 4-6, PSNR values may raise in all compression rates. If we decompose all of three, we will get better performance than decompose only one of them.

Image/rate	Barbara/0.25				
HL		●			●
LH			●		●
HH				●	●
PSNR	27.328	27.3176	27.4761	27.3291	27.51
Image/rate	Barbara/0.5				
HL		●			●
LH			●		●
HH				●	●
PSNR	29.9951	30.0202	30.2534	30.2506	30.53
Image/rate	Barbara/0.75				
HL		●			●
LH			●		●
HH				●	●
PSNR	32.3169	32.315	32.4405	32.6725	32.8101
Image/rate	Barbara/1				
HL		●			●
LH			●		●
HH				●	●
PSNR	34.6112	34.6395	34.7582	34.8979	35.0856

Table. 4-6. Results of 3 subbands decompositions of **Barbara**

Additionally, we also find many images which are very suit to subband decompositions, like **Goldhill** (Fig.4-6 left).... We can get best PSNR value by decomposing LH subband of Goldhill image. Decomposing its HL subband can get good performance, but the performance is not as obvious as we decompose its LH subband. However, it has only tiny ascendant or descendant in HH subband decomposition, and it can scarcely influence performance.

There is a very close relationship between the adaptability of an image fit to be

decomposed and the image content. After our experiments, we find a generally existing fact. Observing edges of the testing image, if there are more horizontal edges than vertical edges, we can decompose **HL subband** to improve the performance. Decomposing other two subbands may decrease PSNR values or make a negligible change. Similarly, if there are more vertical than horizontal edges, we just only decompose **LH subband**. For example, **Straw** image (Fig. 4-10 left) has much vertical edges, and it can be decomposed well by **LH subband**. Decomposing other two may not have improvement. **Boat** (Fig. 4-10 right) image has a large amount of horizontal edge. (See contours of clouds, sea wave and boat) We can find its best decomposition method by **HL subband, too**. If there are fewer vertical, horizontal and diagonal edges, subband decomposition may cause PSNR value a good deal of decreasing. We can see two results showed in Table. 4-7



Fig. 4-10. Straw and Boat

Image/rate	Straw/0.5				
HL		★			★
LH			★		★
HH				★	★
PSNR(dB)	23.6523	23.6563	24.6949	23.6523	24.6962
Image/rate	Boat/0.5				
HL		★			★
LH			★		★
HH				★	★
PSNR(dB)	29.8241	29.9347	29.6594	29.8194	29.75

Table. 4-7. High frequency subband decompositions of Straw and Boat

Expect for Barbara, Straw, and Boat. There are also some images which are suit to be decomposed. They usually have same directional edges than other directions, or with a large amount of texture. For example, Airplane (Fig. 4-11 left) has many vertical edges than horizontal ones, although the body edge of the airplane is almost horizontal. We can decompose its HL subband to enhance PSNR values. Goldhill and Grass (Fig. 4-10 right) have a large amount of detail and texture.

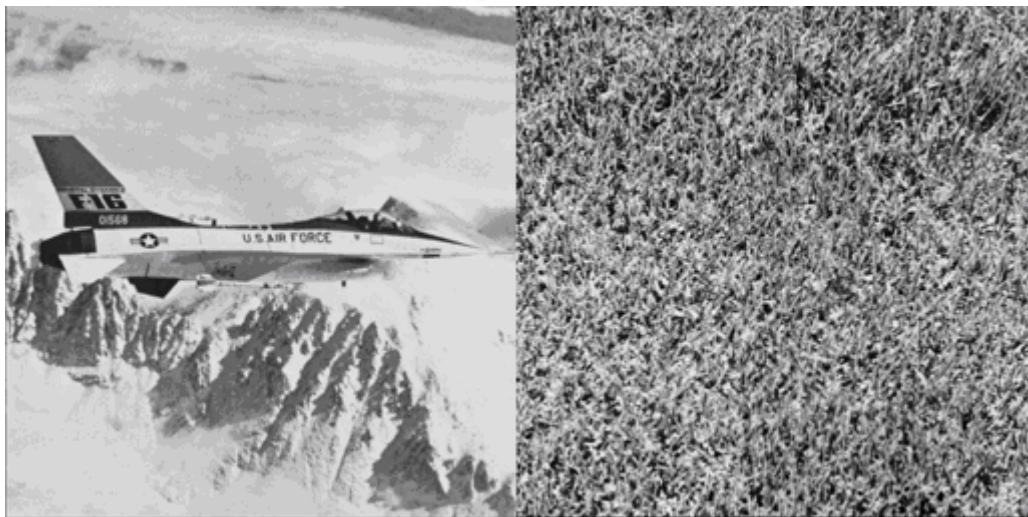


Fig. 4-11. Airplane and Grass

Image/rate	Goldhill/0.5				
HL		●			●
LH			●		●
HH				●	●
PSNR	30.7413	30.7428	30.8225	30.7407	30.8086
Image/rate	Grass/0.5				
HL		●			●
LH			●		●
HH				●	●
PSNR	18.5542	18.548	18.6288	18.5538	18.68
Image/rate	Airplane/0.5				
HL		●			●
LH			●		●
HH				●	●
PSNR	30.53	30.44	30.6282	30.5376	30.34

Table. 4-8. High frequency subband decompositions of Airplane and Grass

This conclusion is similar to previous section. Images with a large amount of texture and detail usually have edges for all directions, and they usually suit to be decomposed. Any subband decomposition may probably improve the PSNR value. In opposition to smooth images, they are often not suit to decompose. However, a smooth image with more edges in the same direction is suit to decompose corresponding subband for reaching the performance improvement.

4.4 Advanced subband decompositions

From Section 4.3, we can find some images which are suit to subband decompositions. This section simulates the method of Section 4.1. LL subband can decompose to highest level (base on image size). If an image has an adaptable high frequency subband can be decomposed, can we decompose it further? For example: if an image has an adaptable LH1 subband, can its LH2 and LH3 subband be still suit to

decompose?

We design some experiments to discuss this appearance.

In order to process our experiments ,we still take two images” **Straw**” and “**Boat**” which are suit to decompose. From the results of previous section, LH subband of Straw image and HL subband of Boat image are suit to decomposed. We proceed to our decomposition test at any rate, and get some data at below Table. 4-9 and 4-10:

Rate/PSNR	Original	LH-LV1	LH-LV2	LH-LV3
0.1	19.4648	19.402	19.6848	19.6848
0.25	21.3559	21.6003	21.9273	21.9273
0.5	23.6523	24.6949	24.8724	24.8701
0.8	26.162	27.257	27.4078	27.4078
1	27.8485	28.968	29.0781	29.0781

Table. 4-9. Higher Level LH subband decompositions of **Straw** with size 256*256



Rate/PSNR	Original	HL-LV1	HL-LV2	HL-LV3
0.1	23.9671	23.9671	23.9699	23.9979
0.25	26.8143	26.809	26.7572	26.8036
0.5	29.8241	29.9347	29.9121	29.9471
0.8	32.5021	32.6206	32.6267	32.6562
1	34.2187	34.3744	34.384	34.4167

Table. 4-10. Higher Level LH subband decompositions of **Boat** with size 256*256

Take Straw image as an example, we can get better PSNR value when we decompose **LH subband** for more times in any compression rate. Even if it does not appear higher performance, its result PSNR will be same as original value. The Boat image also has the same situation. More subband decomposition numbers can reach better performance.

But from this data, we can know that although more decomposition levels can get better results. When we decompose them more times, the improvement of PSNR values will be less obvious. In other words, we can get more PSNR values rising when we decompose HL 2 times than decompose it only one time. But, when we decompose it 3 times, we just get only a little improvement than 2 times. This situation is similar to the results of **Section 4.1**.

In addition, we also test other images which are suit to subband decompositions. We discover a generally existing circumstance. When the compression rate is lower (rate is usually larger than 0.75 bit/pixel), we can decompose high frequency subband to LV2 or upward. By the advantage of energy compacting, we can assure to get better compression results. When we use higher compression rate (rate is usually smaller than 0.25 bit/pixel), even we can not use subband decompositions.

Because energies will be compacted in upper left corner after the subband decomposition, SPIHT compression algorithm will drop more coefficients in high

compression rates. Although energies are compacted, these coefficients will also be dropped. These dropped energies will cause more enormous inaccuracy when we decompress them to the original image. By the same reason, when the rate is 0.5 (we name it “medium compression rate”), we can decompose subband at LV1 or LV2 to get respectable results.

4.5 Using different filter in subband decompositions

4.5.1 Using DCT in subband decompositions

In **Section 3.4.2**, we decide to use 5 levels DCT to decompose subbands of an image. These five levels DCT are 8×8 , 4×4 , 2×2 , 2×2 , and 2×2 DCT. We call it 8-4-2-2-2 DCT method. Because of this decomposition methods can get better effect upon most images. After our tests, we find improved PSNR values when we make use of images which are suit to decompose. For example, texture images, or some natural images, like Barbara, Grass, Goldhill, Straw..., **they can get better PSNR values after 8-4-2-2-2 DCT decomposition in all compression rates**. Therefore, some images which are not suit to decompose also get poor results after this method.

Furthermore, we find some synthesis image, such as Text, Resolution Chart, which do not fit to use this method. Their contents usually have many text or right angles, after extortionate decompositions and restorations, 8-4-2-2-2 DCT method will account for blocking effect. Blocking effect is a weakest point of DCT. When we use DCT in this kind of images, we will get very poor restorations.

Briefly speaking, 8-4-2-2-2 DCT method is suit to texture images or high frequency natural images. Fig. 4-8 shows **Grass** and **House**.

For example, Fig. 4-9 shows 8-4-2-2-2 DCT V.S. Original SPIHT encoder. They are partial enlargement versions of House image with size 256×256 **at ratio 0.8bit/pixel (10:1)**. The left side image is compressed by our method (PSNR=37.91),

and the right side image is compressed by the original SPIHT (PSNR=38.6581). We can easily find that the textures of house bricks of our method are **more distinct** than original SPIHT.

See another sample **Grass** with size 256*256 in **Fig. 4-12**. The upper one (PSNR=21.45) is compressed by 8-4-2-2-2 DCT at **1.0 bit/pixel (8:1)**, the below one (PSNR=21.13) is the original SPIHT at the same rate. In this texture image, our method can reduce some obvious artificial borders and edges.

Table. 4-11 for detail datum. LL subband of all images is worked by Bior 6.8.



Fig. 4-12. Grass and House



Fig. 4-13. 8-4-2-2-2 DCT (left) V.S. Original SPIHT encoder (right)

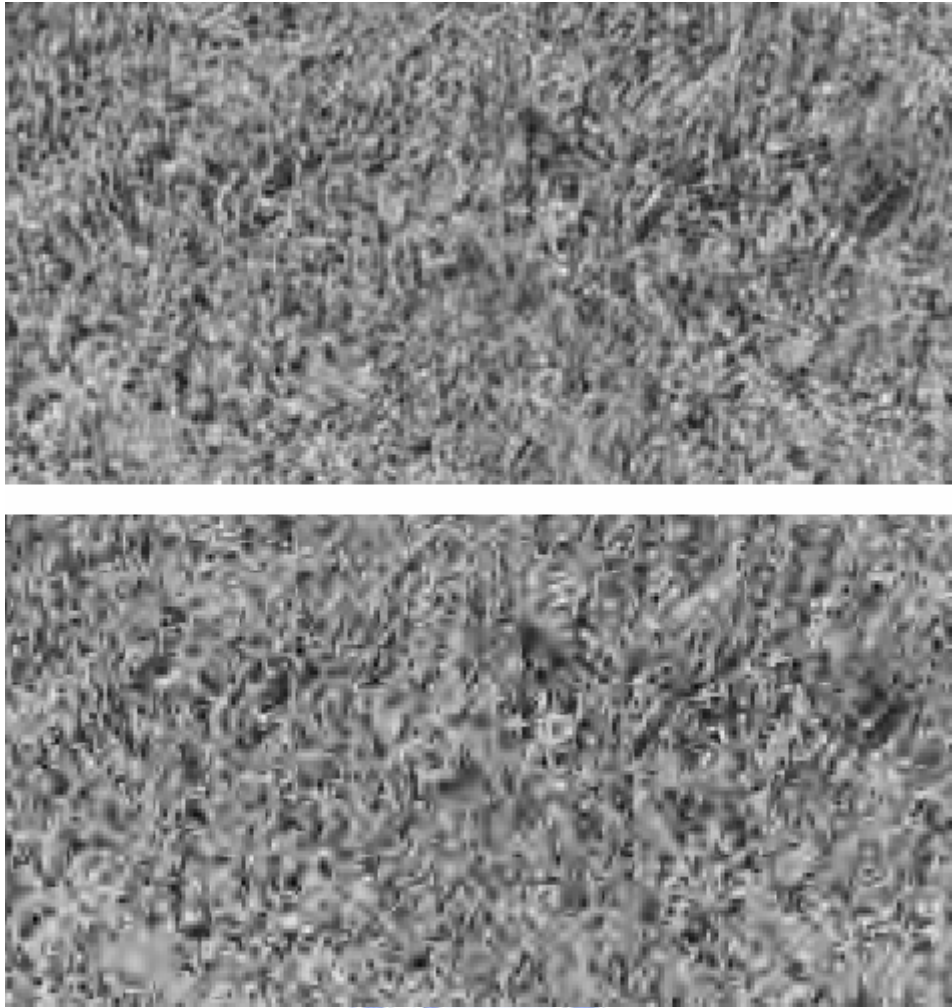


Fig. 4-14. 8-4-2-2-2 DCT (upper) V.S. Original SPIHT encoder (below)

Rate/PSNR	Grass	84222DCT	Goldhill	84222DCT	House	84222DCT
0.1	15.779	15.8001	25.0811	25.1875	27.2352	27.368
0.25	17.0131	17.0443	27.8909	28.0703	31.855	31.8837
0.5	18.5979	18.6236	30.7413	30.9222	35.4384	35.6517
0.8	20.2105	20.4445	33.1969	33.3593	37.9105	38.6581
1	21.1294	21.4515	34.4021	34.6294	39.2406	40.1068

Table. 4-11. Results of original SPIHT and 8-4-2-2-2 DCT

4.5.2 Using different wavelet filter in subband decompositions

In this section, we use the combination testing of different wavelet families and filter orders to HL, LH, and HH subbands which are suit to be decomposed in images.

The results are similar to Section 4.2, different wavelet families and filter orders work

on different subband will get quite distinct outcomes. From Section 4.2 and [5], [7], and [15], **Bi-orthogonal** can work well for LL subband of most images, but it can't work well in other three subbands. **Coiflets** and **Symlets** can decompose other three subbands better than Bi-orthogonal. Sometimes, **dmey**, **Daubechies**, and **Reverse-bi-orthogonal** also can get satisfactory performance. We can use Bi-orthogonal to decompose LL subband very well, but we still can't find a suitable wavelet family which can generally work in other three subbands very well. **Different images get dissimilar results.** Even they are all texture images, they get quite different results.

Because too much factors for us to consider, it is even harder to find an ordinary wavelet which can work well in HL, LH, and HH subbands.

Like **Section 4.2**, we also use 54 wavelets decompose some subbands of particular images. We only list some results of 3 subbands of Barbara image separately. In Table. 4-12, we can't find the regularity of high frequency subband decomposition in Barbara image. Each subband of a specific image gets quite different results. In Table. 4-13, we show only HL subband decomposition results of 3 images Boat, Goldhill, and House. Although they are all HL decomposition, we still can not find their regularity. We just can choose an applicable wavelet family and filter order for particular subband of an image as possible as we can

Barbara at 0.5 b/p high frequency subband decomposition					
HL		LH		HH	
db2	30.1915	coif3	30.3586	dmey	30.4151
sym2	30.1915	coif2	30.3545	sym8	30.4075
db5	30.1856	dmey	30.3537	coif5	30.4073
db3	30.1839	coif4	30.3516	rbio68	30.407
sym3	30.1839	sym5	30.3516	sym6	30.4033
sym5	30.1814	bior68	30.35	db5	30.3981
db4	30.1775	rbio68	30.3498	sym4	30.3957
rbio68	30.173	coif5	30.3453	bior68	30.3945
coif1	30.1718	db5	30.3422	coif4	30.3944
sym7	30.1716	sym4	30.3372	db9	30.3938
coif2	30.1683	sym8	30.337	db4	30.3929
bior68	30.1675	rbio44	30.3345	db6	30.3913
rbio44	30.1669	db4	30.3335	db7	30.3906
rbio55	30.1657	db6	30.3301	sym7	30.3901
coif5	30.1653	db2	30.3291	coif2	30.3897
bior44	30.1643	sym2	30.3291	db8	30.3885
coif3	30.1635	sym6	30.3258	coif3	30.3883
db10	30.1634	bior44	30.3237	db10	30.3815
dmey	30.1622	db9	30.3226	rbio44	30.3804
sym6	30.162	db3	30.3154	bior44	30.3775

Table. 4-12. Barbara at 0.5 b/p high frequency subband decomposition

Only HL subband decomposition					
of Boat, Goldhill, and House at 0.5 b/p					
Boat		Goldhill		House	
dmey	29.9454	coif2	30.7987	sym6	35.5489
rbio68	29.944	coif3	30.7974	sym4	35.5416
sym8	29.9356	sym5	30.7853	sym8	35.5347
bior68	29.9347	bior13	30.7767	coif3	35.5275
sym7	29.9318	rbio13	30.7767	dmey	35.5184
coif2	29.9298	bior11	30.771	coif4	35.5119
sym4	29.9294	rbio11	30.771	rbio68	35.5097
sym6	29.9282	db1	30.771	bior55	35.5085
coif1	29.9269	sym1	30.771	db5	35.4869
rbio44	29.9266	coif1	30.7675	coif5	35.4856
coif5	29.925	bior15	30.7668	sym7	35.4843
db3	29.923	rbio15	30.7668	coif2	35.4773
sym3	29.923	sym4	30.7542	db4	35.4773
sym5	29.9186	sym7	30.7541	db3	35.4743
db6	29.9182	db4	30.754	sym3	35.4743
bior44	29.9162	db2	30.7538	bior68	35.4687
db7	29.9161	sym2	30.7538	rbio13	35.4653
coif4	29.9144	sym6	30.7537	db7	35.4582
coif3	29.91	coif4	30.7507	rbio15	35.4561
db2	29.9084	coif5	30.7489	rbio26	35.4468

Table. 4-13. Only HL subband decomposition of Boat, Goldhill, and House at 0.5 bit/pixel

When we decompose LL subband, using an appropriate wavelets will get more obvious improvement. There is less evident difference for choosing suitable wavelets in other three high frequency subbands. So, choosing wavelets has less importance in high frequency subbands than it in LL subband.

4.6 Final experimental results

Combining methods of previous sections, we use our proposed algorithm to compress Barbara image with size 512*512, and to compare with other well-known compression algorithms, like SPIHT, SLCCA, MRMD, and JPEG..

See Table. 4-14 for final results. In **Section 3.4.1**, we decompose Barbara image with size 512*512 for LV9 LL subband by using Bior6.8, and decompose HL by using **Rbio6.8**, LH by **coif5** and HH by **dmey**. Final results show that when we use higher compression rate (**rate is below 0.25**), **LV2** high frequency decomposition will get best performance (See Proposed LV2). When the rate is **above 0.5**, we can decompose high frequency subbands to **LV3** in order to get best PSNR values. (See Proposed LV3)

Fig. 4-15 indicates that our proposed can improve some details. They are partial enlargement versions of Barbara image with size 512*512 **at ratio 0.25 bit/pixel (32:1)**. The left side image is compressed by our method (PSNR=28.28), and the right side image is compressed by the original SPIHT (PSNR=27.57). We only mark some differences of these two compressed images. See the black rectangles, improved details will be observed.

In **Section 3.4.2**, we propose a decomposition method: 8-4-2-2-2 DCT, and also show its result in Table. 4-14. For some images which are suit to decompose, it is also an improve method.

Comparing with other algorithms, we also can get better PSNR values than other well-known compression algorithms. For all compression rates, our proposed method can get about 0.4-0.7 PSNR values increasing than SPIHT, about 0.1 than SLCCA, about 0.5 than MRMD.



Fig. 4-15. Our proposed (left) can improve some details

256 gray level Barbara image with size 512*512

Rate/Algo	SPIHT	SLCCA	MRMD	JPEG	84222DCT	ProposedLV1	ProposedLV2	ProposedLV3
0.1					24.6037	24.4658	24.7603	24.7346
0.125	24.84	25.36	25.27	22.9	25.1788	25.0607	25.3875	25.3468
0.25	27.57	28.18	27.86	25.2	27.8447	27.8655	28.2816	28.2434
0.5	31.39	31.89	31.44	28.3	31.5831	31.706	32.01	31.9834
0.75	34.3	34.6	34.2	31.6	34.2539	34.338	34.6823	34.6934
1	36.41	36.69	36.24	33.1	36.4207	36.5736	36.7903	36.8067

Table. 4-14. Final results of Barbara with size 512*512, our proposed LV1, 2, and 3 and 8-4-2-2-2 DCT and other well-known compression algorithms



CHAPTER 5

Conclusions and Future Works

5.1 Conclusions

In this paper, we propose some methods which can enhance image compression performance. Characteristics of our proposed method include the following:

1. Our methods can work on some images very well and get better PSNR values than other famed compression algorithms. But these images must be suit to be decomposed.

2. We propose the other method “8-4-2-2-2 DCT” which use DCT to decompose images. It can also improve compression performance, but it sill must work on images which are suit to be decomposed.

3. Observing edges of the testing image, if there are more **horizontal** edges than vertical edges, we can decompose **HL subband** to improve performance.

Decomposing other two subbands may decrease PSNR values or make a negligible change. Similarly, if there are more **vertical** than horizontal edges, we just only decompose **LH subband** and so forth. Images with a large amount of texture and detail usually have edges for all directions, and they usually suit to be decomposed.

4. There are too much factors need to be consider. We can't find a best solution to fit all kinds of images. Some synthesis images and low activity natural images do not suit to be decomposed.

5. About some methods proposed by other papers, we also analysis and compare them, and get some conclusions. SPIHT encoder can get best performance by decomposing LL subband more and more times. Whether other encoder has this situation is uncertain.

Bi-orthogonal wavelet can get better performance to work on most images, but we

also find it can't work on high frequency subbands very well. Other wavelets are more suitable than Bi-orthogonal one.

5.2 Future Works

By conclusion 4, we still can't find a suitable method to decompose images "adaptively". This "adaptive" method can decompose high frequency subbands of particular image by its properties. These properties include decomposition numbers, compression ratios, wavelet families and filter orders... We can determine whether a subband can be decomposed or not by using directions of edges, but how to measure comparative directional numbers is still an un-solvable problem.



References

- [1] Liagrui Tang ,Jing-ao Sun,and Anni Cai,“An Improved Zerotree Wavelet Image Compression Method ,” *Proceedings of ICSIP2000 IEEE*
- [2] Michael B. Martin and Amy E.“New Image Compression Techniques Using Multiwavelets and Multiwavelet Packets,” *IEEE Transactions on Image Processing, VOL. 10, NO. 4, April 2001*
- [3] B.B.Chai ,J.Vass, and X. Zhuang, “Significance-linked connected component analysis for wavelet image coding,” *IEEE Transactions on Image Processing. Vol.8,No. 6,Jun. 1999,pp. 774-784.*
- [4] Bryan E. Usevitch “A Tutorial on Modern Lossy Wavelet Image Compression: Foundations of JPEG 2000,” *IEEE Signal Processing Magazine September 2001*
- [5] Sonja GrgC, Mislav GrgiC, Branka Zovko-Cihlar, “OPTLMAL DECOMPOSITION FOR WAVELET IMAGE COMPRESSION,” *First Int'l Workshop on Image and Signal Processing and Analysis, June 14-15, 2000. Pula, Croatia*
- [6] Jia Wang, Wenjun Zhang and Songyu Yu,” Wavelet coding method using small block DCT,” *ELECTRONICS LETTERS 10th May 2001 Vol. 37 No 10*
- [7] Sonja Grgic, Mislav Grgic, *Member, IEEE*, and Branka Zovko-Cihlar, *Member, IEEE*, “Performance Analysis of Image Compression Using Wavelets,” *IEEE Transactions on Circuits and Systems for Video Technology, VOL. 48, NO. 3, June 2001*
- [8] Fang Zhijun, Zhou Yuanhua, Zou Daowen,” A Scalable Video Coding Algorithm Based DCT-DWT,” *Inst. of Image Comm. & Info. Processing Shanghai Jiaotong Univ.*
- [9] Junqiang Lan ,Xinhua Zhuang,” Embedded Image Compression Using DCT

- Based Subband Decomposition and SLCCA Data Organization,” *2002 IEEE*
- [10] Ian Rice” SET PARTITIONING ALGORITHMS FOR WAVELET BASED IMAGE COMPRESSION,” *IEEE November 2004*
- [11] Gregory K. Wallace ” THE JPEG STILL PICTURE COMPRESSION STANDARD,” *IEEE Transactions on Consumer Electronics, Vol. 38, No. 1, FEBRUARY 1992*
- [12] Michael W. Marcellin, Michael J. Gormish, Ali Bilgin¹, Martin P. Boliek,” An Overview of JPEG-2000,”*IEEE*
- [13] Zixiang Xiong, Kannan Ramchandran, Michael T. Orchard, and Ya-Qin Zhang,” A Comparative Study of DCT- and Wavelet-Based Image Coding,” *IEEE Transactions on Circuits and Systems for Video Technology, VOL. 9, NO. 5, AUGUST 1999*
- [14] Wonyong Chong, Jongsoo Kim,” Speech and Image Compressions by DCT, Wavelet, and Wavelet Packet,” *International Conference on Information, Communications and Signal Processing ICICS '97 Singapore, 9-12 September 1997*
- [15] Wei-Ting Kao, “Analyses and Comparisons of Image Compression by Wavelets,” *National Chiao Tung University 2005*
- [16] Marta Bertran Pardo and Christian Tenllado van der Reijden “Embedded lossy image compression based on wavelet transform,”*VIPromCom-2002,4th EURASIP-IEEE Region 8 international Symposium on Video/Image Processing and Multimedia Communications, 16-19 June 2002*
- [17] M. Grgic, M. Ravnjak, and B. Zovko-Cihlar, “Filter comparison in wavelet transform of still images,” *in Proc. IEEE Int. Symp. Industrial Electronics, ISIE'99, Bled, Slovenia, 1999, pp. 105–110.*
- [18] S. Grgic, K. Kers, and M. Grgic, “Image compression using wavelets,”*in Proc.*

IEEE Int. Symp. Industrial Electronics, ISIE'99, Bled, Slovenia, 1999, pp. 99–104.

- [19] M. K. Mandal, S. Panchanathan, and T. Aboulnasr, “Choice of wavelets for image compression,” *Lecture Notes Comput. Sci.*, vol. 1133, pp. 239–249, 1996.
- [20] R. R. Coifman, Y. Meyer, and M. V. Wickerhauser, “Wavelet analysis and signal processing, in Wavelets and Their Applications,” *Boston, MA: Jones and Bartlett, 1992, pp. 153–178.*
- [21] Qu JiShuang, Wang Chao “A wavelet package-based data fusion method for multitemporal remote sensing image processing,”*2001 CRISP,SISV,AARS*
- [22] Hiroshi KONDO and Hiroki KOU “Wavelet Image Compression using Sub-block DCT,”*2001 IEEE*
- [23] Ricardo de Queiroz, C.K. Choi, Young Huh, and K. R. Rao ”Wavelet Transforms in a JPEG-like Image Coder,” *IEEE Transactions on Circuits and Systems for Video Technology* ,VOL.7 No2,1997 April
- [24] Amir Said,William, A. Pearlmann“A New , Fast, and Efficient Image Codec Based on Set Partitioning in Hierarchical Tress,” *IEEE Transactions on Circuits and Systems for Video Technology* ,VOL.6 No3,1996 June
- [25] J.M.Shapiro,”Embedded image coding using zerotrees of wavelet coefficients,”
IEEE TRANSACTIONS ON Signal Processing Vol. 41, No,12, Dec.1993